Microbiology and Infectious Disease

DNA Methylome Regulates Virulence and Metabolism in *Pseudomonas syringae*

Reviewed Preprint
v2 • February 4, 2025
Revised by authors

Reviewed Preprint
v1 • April 12, 2024

Jiadai Huang, Fang Chen, Beifang Lu, Yue Sun, Youyue Li, Canfeng Hua, Xin Deng

Department of Biomedical Sciences, City University of Hong Kong, Hong Kong, China • Shenzhen Research Institute, City University of Hong Kong, Shenzhen, China • Tung Research Centre, City University of Hong Kong, Hong Kong SAR, China • Chengdu Research Institute, City University of Hong Kong, Chengdu, China

eLife Assessment

This **valuable** study presents findings on DNA methylation as an efficient epigenetic transcriptional regulating strategy in bacteria. The authors utilized single-molecule real-time sequencing to profile the DNA methylation landscape across three model pathovars of Pseudomonas syringae, identifying significant epigenetic mechanisms through the Type-I restriction-modification system, which includes a conserved sequence motif associated with N6-methyladenine. The evidence presented is **solid** and the study provides novel insights into the epigenetic mechanisms of P. syringae, expanding the understanding of bacterial pathogenicity and adaptation.

https://doi.org/10.7554/eLife.96290.2.sa3

Abstract

Bacterial pathogens employ epigenetic mechanisms, including DNA methylation, to adapt to environmental changes, and these mechanisms play important roles in various biological processes. *Pseudomonas syringae* is a model phytopathogenic bacterium, but its methylome is less well known than that of other species. In this study, we conducted single-molecule real-time sequencing to profile the DNA methylation landscape in three model pathovars of *P. syringae*. We identified one Type-I restriction-modification system (HsdMSR), including the conserved sequence motif associated with N^6-methyladenine (6mA). About 25%–40% of the genes involved in DNA methylation were conserved in two or more of the strains, revealing the functional conservation of methylation in *P. syringae*. Subsequent transcriptomic analysis highlighted the involvement of HsdMSR in virulent and metabolic pathways, including the Type III secretion system, biofilm formation, and translational efficiency. The regulatory effect of HsdMSR on transcription was dependent on both strands being fully 6mA methylated. Overall, this work illustrated the methylation profile in *P. syringae* and the critical involvement of DNA methylation in regulating virulence and metabolism. Thus, this work contributes to a deeper understanding of epigenetic transcriptional control in *P. syringae* and related bacteria.

Introduction

Pseudomonas syringae inflicts leaf spots and cankers on plants globally, and its adequate control poses significant challenges. More than 60 pathovars have been identified, which infect almost all economically important crops in the world (1, 2). *P. syringae* pv. *phaseolicola* 1448A (*Psph*), one of the classical strains of *P. syringae*, can cause severe halo blight of common beans (*Phaseolus vulgaris*), which raises it from a common pathogen to a molecular plant-pathogen bacterium(3). *P. syringae* pv. *tomato* DC3000 (*Pst*) and *P. syringae* pv. *syringae* B728a (*Pss*) are two other model strains whose natural host plants are tomatoes and beans, respectively (4, 5). The most important weapon of *P. syringae,* and the first to be characterised, is the Type III secretion system (T3SS) encoded by *hrp* and *hrc* gene clusters, which are flanked by the conserved effector locus and deliver T3 effectors into host cells (6).

The expression of T3SS genes is inhibited in nutrient media such as King's B (KB), whereas it is induced in minimal medium or plant cells (7–9). The HrpRSL pathway is the primary regulator of the T3SS in *P. syringae*, with HrpRS activating *hrpL* expression. HrpL then binds to the *hrp* box to induce the translation of downstream T3 effectors (10–12). HrpRSL also impacts other virulence-related mechanisms, including motility, biofilm formation, siderophore production, and oxidative stress resistance, which are under the control of complicated regulatory networks, allowing *P. syringae* to infect plants (13–19). However, the methylome and function of DNA methylation in *P. syringae* pathogenesis and metabolism remain largely unknown.

In bacteria, DNA methylation is the primary level of epigenetic regulation because these prokaryotes lack the histones and nucleosomes of eukaryotic cells. Bacterial DNA has three primary forms of methylation: N^6-methyladenine (6mA), N^4-methylcytosine (4mC), and N^5-methylcytosine (5mC). The latter is the most common type in eukaryotes, while 6mA is the dominant form in prokaryotes. DNA methylation in bacteria is mainly the product of methyltransferase (MTase) enzymes, which transfer a methyl group from S-adenosyl-l-methionine to various positions on target bases, depending on the modification (20). MTases originate from the restriction-modification (R-M) system, which protects bacterial cells from invading DNA by recognising and cleaving specific unmethylated motifs (21, 22). There are three main types of R-M systems, Types I, II, and III, categorised according to the related subunits and the precise site of DNA restriction (23, 24). Additionally, orphan MTases are an emerging group of MTases without cognate restriction that are involved in the regulation of DNA replication and gene expression (21). The Type I R-M system contains three host-specificity determinant (*hsd*) subunits, restriction (R), modification (M), and specificity (S), which are encoded by *hsdR*, *hsdM*, and *hsdS*, respectively. Genome sequencing and bioinformatics analyses have revealed that the HsdMSR system exists in around half of all bacteria and archaea species (24). Nonetheless, the biological roles and specific motifs alongside their targets of most MTases remain unknown, especially those related to 6mA (25).

A new sequencing technology, single-molecule real-time (SMRT) sequencing, can detect all three forms of DNA methylation, but particularly 6mA (26). SMRT-seq has been applied for complete genome sequencing and insertion sequence profiling in different *P. syringae* pv. *actinidiae* (*Psa*) strains (27–29). In *P. aeruginosa*, Type I R-M systems, along with their specific motifs, have been identified in the model strain PAO1 and two clinical strains via SMRT-seq. These MTases are considered to play important roles in *P. aeruginosa* virulence or drug resistance (30–32).

To study the targets and functions of DNA modifications in *P. syringae*, SMRT-seq was used to identify global methylation sites and reveal their conserved and divergent functions in the three model strains in this study. We found that HsdMSR in *Psph* was involved in modulating three pathways, namely T3SS, biofilm production, and the metabolism-related gene expression of

ribosomal proteins. Moreover, we found that HsdMSR-mediated transcriptional regulation depends on the full methylation of both DNA strands. Taken together, our results provide insights into the involvement of DNA methylation in the phenotypic traits of *P. syringae* and transcription regulatory mechanisms that may apply to other pathogenic bacteria.

Results

Genome-wide methylome profiling of three model *P. syringae* strains

According to REBASE (33) database prediction, 0 to 2 Type I R-M systems and 3 to 4 Type II R-M systems exist in the three pathovars of *P. syringae*, indicating that Type I is more conserved than Type II in this pathogen (Table S1). To characterise their methylomes, we performed SMRT-seq to obtain the methylation patterns on a genome-wide scale using DNA extracted from the stationary phase of the three wild-type (WT) strains. Our results revealed a total of 10,302 modified bases, of which 3,849, 4,646, and 1,807 nucleotides were significantly identified as being 6mA, 5mC, and 4mC modified, with an interpulse duration ratio (IPD) of > 1.5 throughout the genome of *Psph* (**Fig. 1A**). After identifying the significantly modified sites, we orientated the gene locus tags within the methylated bases. Most genes harboured only 6mA modifications, although 339 genes harboured all three DNA methylation types (**Fig. 1B**).

In *Pst*, a total of 6,002, 2,242, and 3,514 methylation sites were significantly identified as 6mA, 4mC, and 5mC, respectively, using the same cut-off (IPD >1.5) (**Fig. 1C**). Among these modified bases, more genes equipped with all three modification types were detected in *Pst* than *Psph*, with 591 (17.7%) genes exhibiting modifications in *Pst* sequences (**Fig. 1D**). Additionally, the methylome atlas of *Pss* revealed a lower incidence of methylation than those of *Psph* and *Pst*, particularly in terms of 6mA modifications, which were only seen in 457 significant 6mA occurrences under the same threshold (IPD > 1.5) and a total of 2,853 and 1,438 methylation sites were detected as 5mC and 4mC, respectively (**Fig. 1E**). Comparative analysis of the three methylations in *Pss* showed that the highest numbers of genes were modified by 4mC and 5mC simultaneously (**Fig. 1F**).

Characteristics of modified loci and GC contents in *P. syringae*

To further uncover the distribution of the modifications throughout the genome, we calculated how many of the three kinds of modified sites were in these three strains. The majority of modifications occurred in coding sequence (CDS) regions, accounting for at least 80% (Fig. S1A), and less than 20% were in intergenic regions and non-coding RNA (tRNA and rRNA). However, compared with 4mC and 5mC, 6mA was more likely to be in intergenic regions, which suggests that it potentially functions in transcription regulation in *P. syringae*.

It is known that 5mC occurs within CpG sites in CpG islands, which contain higher GC percentages than is typical in the human genome (34). Additionally, the GC architecture can influence DNA methylation in eukaryotic cells (35). To determine the GC content characteristics of modification sites in *P. syringae*, we extracted the sequences 50-bp upstream and downstream from the modified bases and calculated their GC content. The distribution of modification sites and their GC content are shown in density plots. Compared with 4mC and 5mC, the GC contents of 6mA sites were the lowest and the closest to the average GC percentage of *P. syringae* (58% for *Psph* and *Pst*, 59.2% for *Pss*) (Fig. S1B). In contrast, 5mC modification bases had the highest GC content, especially in *Pss* (Fig. S1C). Furthermore, 4mC sites in *Psph* had a higher GC content than those in *Psa* and *Pss* (Fig. S1D). Similar phenomena have been observed in various other bacterial species. For instance, the *Escherichia coli* MTase Dcm can catalyse the 5'CCWGG3' motif (36). Furthermore, in *Spiroplasma* sp. strain MQ-1, more than 95% of 5mC modifications are found in high-CG sequences, which is similar to the pattern in eukaryotes (37).

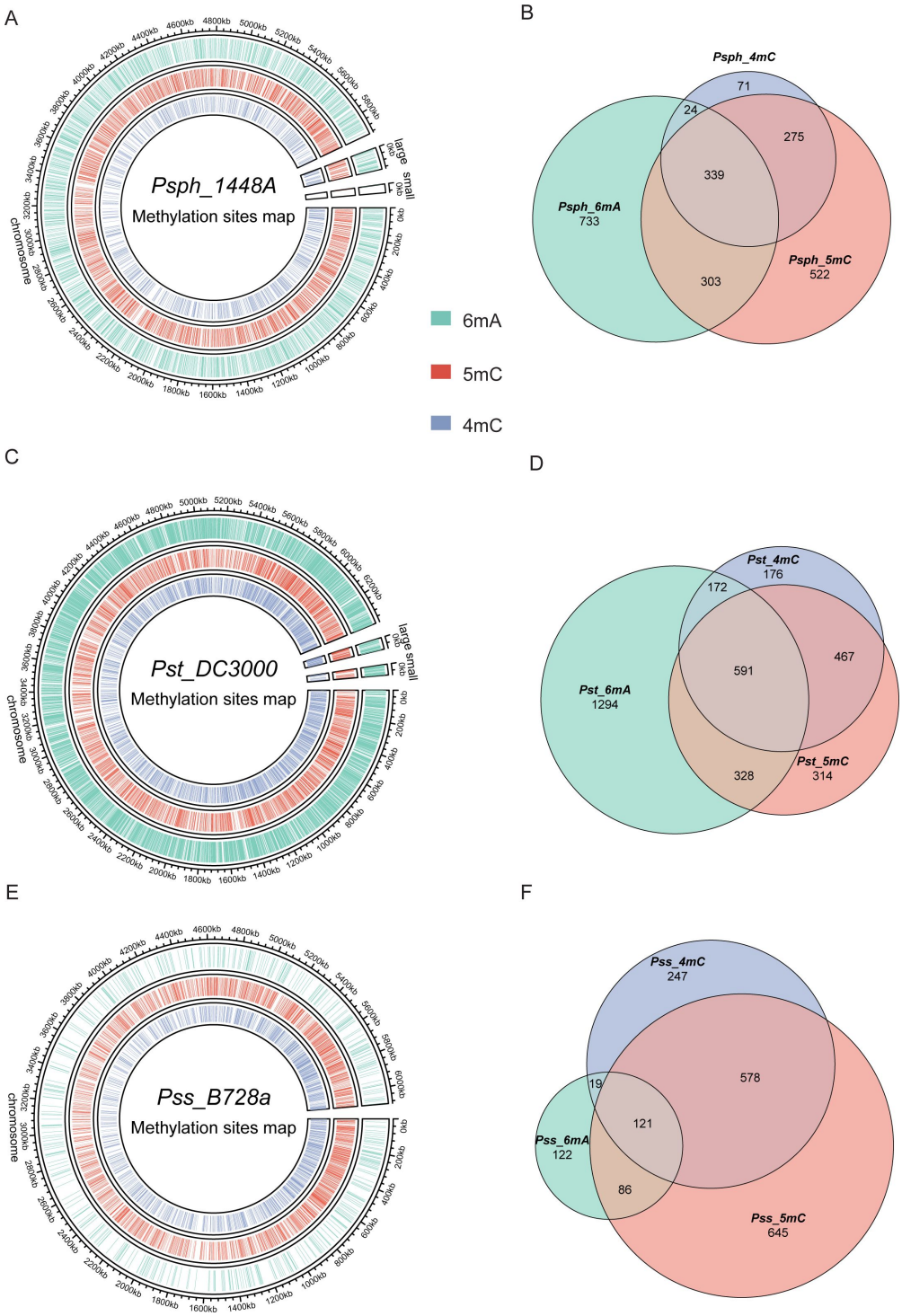

Figure 1.

Genome-wide identification of *P. syringae* DNA methylation.

(A) The circle map displays the distribution of 6mA, 5mC, and 5mC in *Psph* WT. **(B)** The Venn plot reveals overlapped genes within three types of DNA methylation of *Psph* WT. **(C)** The circle map displays the distribution of 6mA, 5mC, and 5mC in *Pst* WT. (**D**) The Venn plot reveals overlapped genes within three types of DNA methylation of *Pst* WT. **(E)** The circle map displays the distribution of 6mA, 5mC, and 5mC in *Pss* WT. **(F)** The Venn plot reveals overlapped genes within three types of DNA methylation of *Pss* WT.

Methylated genes are functionally conserved among three *P. syringae* strains

When we compared the three methylation types in the three tested strains, we observed the conservation pattern among them (**Fig. 2A-B**) and Table S2). Notably, about 25% to 45% of methylated genes were conserved in two and three strains. Interestingly, 5mC had the highest conservation level (39.1%), which might be explained by the rare occurrence of 6mA in *Pss*. Conversely, an obviously higher degree of conservation was observed in virulence-related genes, including T3SS and alginate biosynthesis-related genes, between *Psph* and *Pst* (Table S2). Additionally, some methylated genes (n = 739) harboured sites for different modification types in the three strains (**Fig. 2A**). For example, the modification sites of a Cro/CI family transcriptional factor (TF) in PSPPH_1319 were for different modification types in the three *P. syringae* strains. The Cro/CI are important TFs present in phages. The interaction between Cro and CI affects bacteria immunity status in Enterohemorrhagic *Escherichia coli* (EHEC) strains (38). *Psph* carried 6mA and 5mC, while *Pst* and *Pss* had 5mC and 4mC. This difference might result from differences in the MTases and their specific motifs (Table S2).

To elucidate the functions of genes methylated with these three modification types, functional enrichment analyses were performed based on gene ontology (GO) and Kyoto Encyclopedia of Genes and Genomes (KEGG) databases (39, 40). Analysis revealed the shared functional characteristics of genes with 5mC and 4mC modifications in *Pss* and *Pst*. In contrast, genes with 6mA modifications exhibited more conserved functional terms between *Psph* and *Pst* (**Fig. 2C**). For instance, *Pst* and *Pss* contained 4mC-methylated genes enriched in signalling transduction and TF binding, whereas *Psph* exhibited enrichment in oxidation–reduction process and nucleic acid binding genes. Remarkably, notable conservation of functional terms was observed for genes with 6mA modifications, with at least 21 terms conserved between *Psph* and *Pst*. These terms included ATP binding, catalytic activity, integral component of membrane, transferase activity, and phosphorylation. We also conducted Cluster of Orthologous Group (COG) protein function analysis (41, 42), which assigned the methylated genes from the three strains to 20 categories with diverse functions (Fig. S2A-C). In *Psph*, the top three COG classifications encompassed inorganic ion transport, amino acid transport, and transcription (Fig. S2A). Furthermore, the abundance of modified genes related to cell wall/membrane/envelope biogenesis (M category) in *Pss* was lower than that of *Psph* and *Pst*. Despite the slight variations in COG distribution, the overall pattern exhibited considerable similarity and conservation across the three strains.

Five conserved sequence motifs of 6mA and 4mC were identified in *P. syringae*

Obtaining the whole methylomes of the three strains led us to investigate the associated MTases and their target motifs. The PacBio motif finder and MEME suite (43) were used to determine the specific sequence motifs within 50 bp upstream and downstream of the significantly modified bases. Using the results of both software packages with corresponding cut-offs, we identified two 6mA motifs in *Psph:* C**A**GCN($_6$)CTC and RAGT**A**CTY (**Fig. 3A**). The bolded bases indicate the methylation sites in these motifs. The two motifs occurred a total of 2,998 and 300 times in double strands, and more than 98% and 77% of those occurrences were methylated, respectively, revealing the high methylation rates of these two motifs and implying their crucial roles in *Psph* (**Fig. 3B**). However, the analysis did not obtain any identified motifs for cytosine modifications.

Three motifs for 6mA and one motif for 4mC were identified in *Pst* (**Fig. 3C**). The first 6mA motif, CAARG**A**A, was found 2,022 times in the genome, with 2,019 of the occurrences methylated (99.8%) (**Fig. 3D**). The second 6mA motif, G**A**AN($_4$)RTRCC, was fully methylated in both strands. Similarly, the last 6mA motif, GY**A**GN($_5$)CTRC, exhibited a high methylation level (96%) in the genome of *Pst*. Conversely, the only motif identified for 4mC in *Pst* displayed a considerably lower

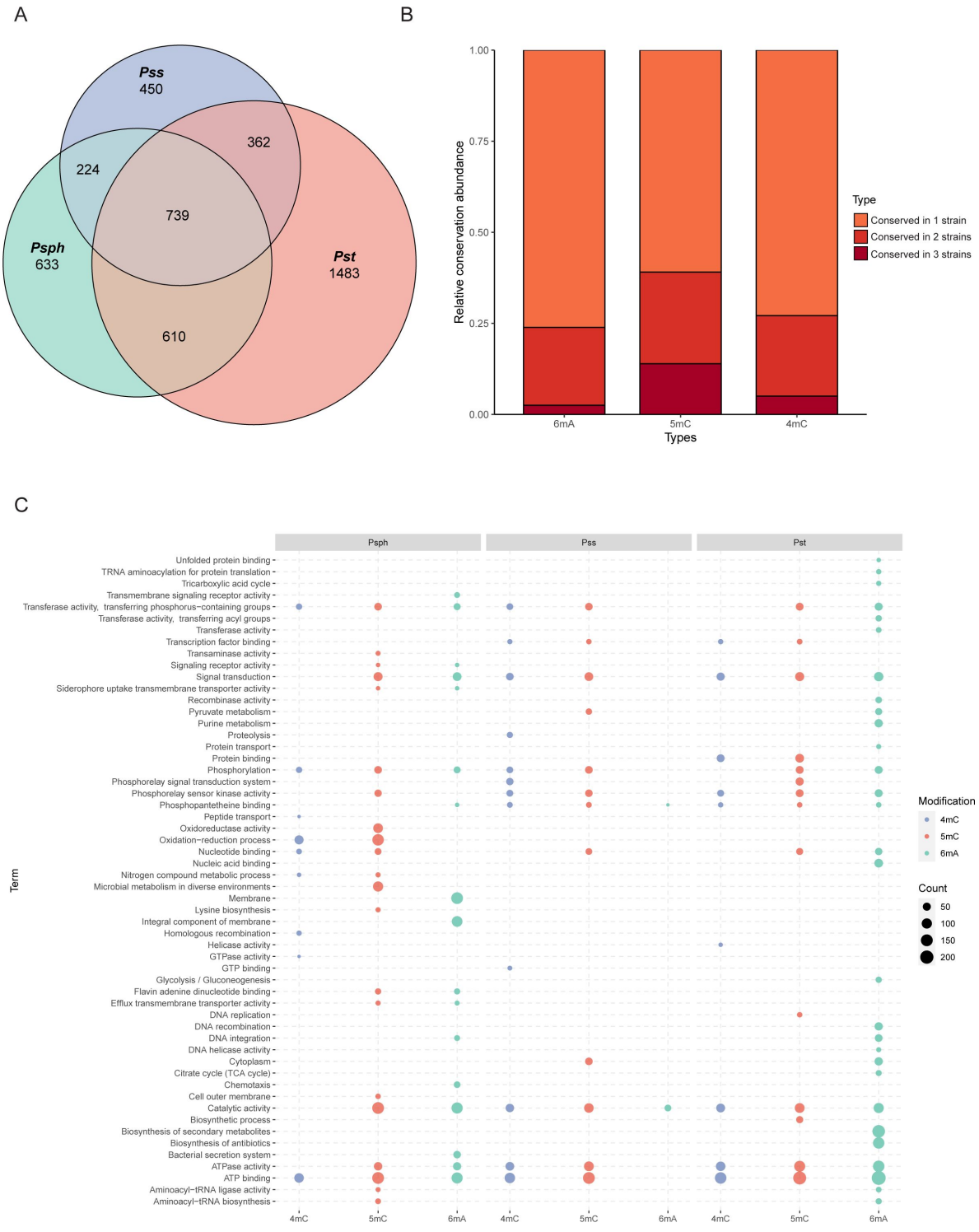

Figure 2.

Functional enrichment analysis of methylation sites in three *P. syringae* strains.

(A) Repartition of the total pool of modified genes among strains. **(B)** Proportion of methylated genes detected in one, two, or three genomes for all *P. syringae* strains and conserved DNA methylation sites with detected genes. **(C)** The dot plot revealed the significantly enriched functional pathways in GO and KEGG databases among three *P. syringae* strains. The specific names of each pathway were listed on the left, and each column with dots indicated the number of genes within one kind of methylation in one of three *P. syringae* strains. The size of the dots indicates the number of related genes.

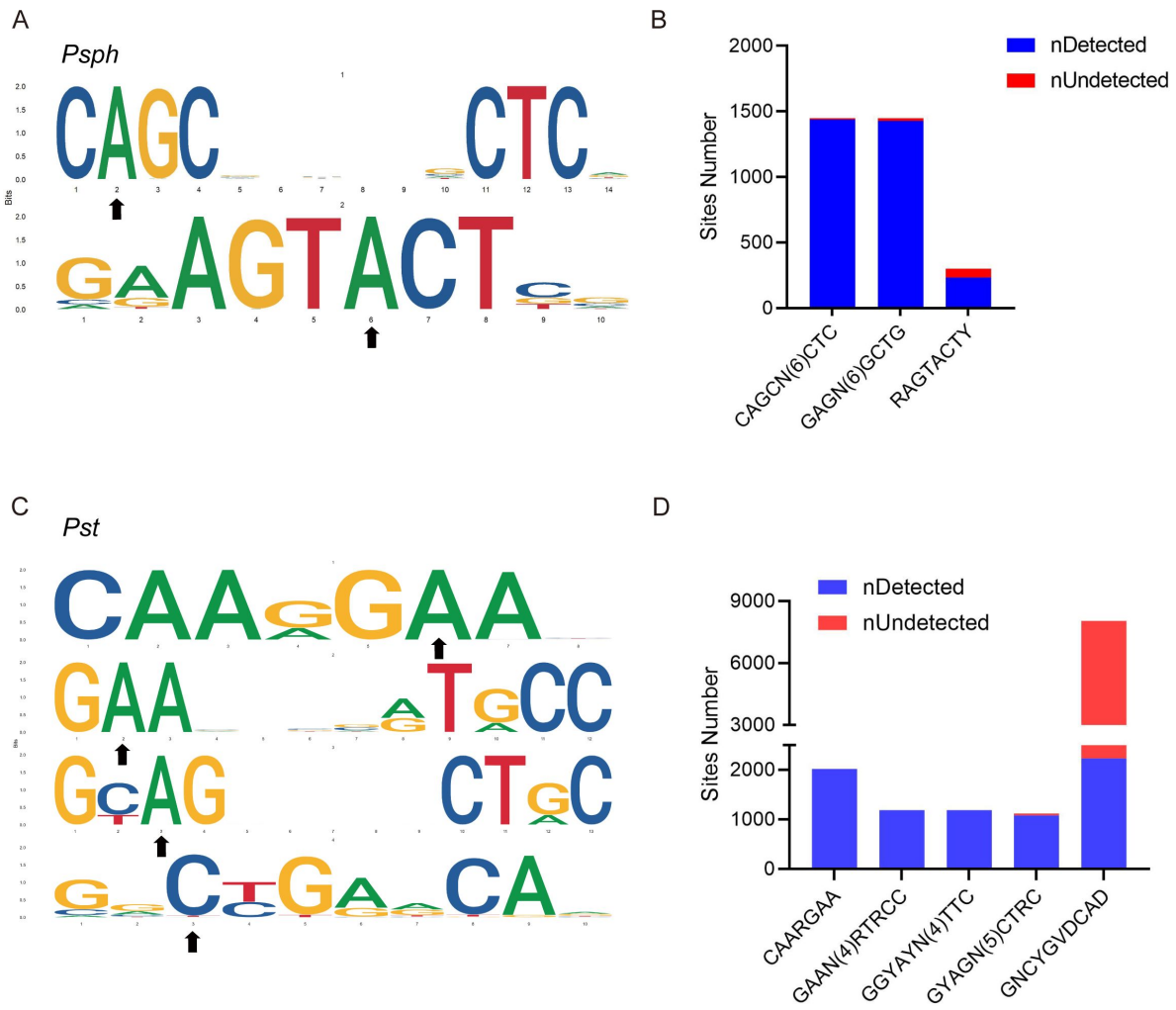

Figure 3.

DNA methylation motifs in *P. syringae*.

(A) 6mA methylation motifs found in *Psph* using SMRT-seq. The black arrows indicate the site of adenine methylation. **(B)** Bar plot shows the abundance of methylated numbers throughout all motif sites in *Psph*. **(C)** 6mA and 4mC methylation motifs found in *Pst* using SMRT-seq. The black arrows indicate the site of base methylation. **(D)** Bar plot shows the abundance of methylated numbers throughout all motif sites in *Pst*.

methylation level than the 6mA sites, with 2,207 occurrences of methylation out of a total of 8,048 sites (approximately 27%). Notably, no credible motifs were found in *Pss* because of its noticeably lower modification levels compared with the other two strains. Overall, the application of SMRT-seq to the three model *P. syringae* strains identified specific sequence motifs, including 6mA motifs, exhibiting extensive methylation statuses.

In vivo validation revealed the activity and specificity of Type I R-M system MTase in *Psph*

The first motif, C**A**GCN($_6$)CTC, identified in *Psph* is similar to the counterpart modified by a Type I R-M MTase in *P. aeruginosa* (26) (Fig. S3), suggesting that the putative HsdMSR is responsible for the observed motif. As no other motifs exhibited a discernible association with the Type II R-M MTases, we opted to focus our investigation on the putative HsdMSR in *Psph.* To determine the potential functions of the putative MTases, we constructed MTase knock-out mutants and complementary strains of HsdMSR. Growth curve experiments showed the adverse effects on Δ*hsdMSR* compared to the WT strain (Fig. S4A). To confirm the activity of HsdMSR, a dot blot assay was used to detect the 6mA intensity in WT and Δ*hsdMSR*. The results shown in Figure S4B illustrated that 6mA levels were significantly decreased in Δ*hsdMSR* compared to the WT, but were restored in the complemented strain. In addition, SMRT-seq was performed on Δ*hsdMSR*, which further profiled methylation patterns in Δ*hsdMSR* (Fig. S4C-D). As expected, we found almost all of the reduction 6mA sites in the Δ*hsdMSR* were from motif CAGCN(6)CTC (Fig. S4E-F). We also noticed that 5mC and 4mC sites in the mutant were relatively similar to that in WT (Fig. S4E), and the slight difference might be caused by sequencing errors. Overall, we propose that HsdMSR only catalyze the 6mA located on the motif CAGCN(6)CTC, but does not affect other 6mA sites and other modification types.

In accordance with previous studies showing that growth conditions affect the bacterial methylation status (44–46), we applied dot blot experiments using the same amount of DNA (1 μg) from these three *P. syringae* strains to detect the 6mA levels during both logarithmic and stationary phases. The results revealed that 6mA levels in the stationary phase were much higher than those in the logarithmic phase in *Psph* and *Pst*, but no significant change in *Pss* (Fig. S5A). Additionally, we found that during the stationary phase, 6mA methylation levels in *Psph* and *Pst* were higher than those in *Pss*. These findings were consistent with the MTases predication on these three strains since *Pss* does not harbor any type I R-M systems, which are important for 6mA medication in bacteria. We also overexpressed HsdM in *Pst* and performed additional experiments in WT and the HsdM overexpression strains, including dot blot and growth curve assays. The results showed that the MTase overexpressed strain presents a higher 6mA level than WT during the logarithmic phase, and the overexpression of MTase had no effects on growth in *Pst* (Fig. S5B-C). Taken together, the results demonstrated that 6mA levels change with the bacterial growth phase in *Psph* and *Pst*, and HsdMSR is responsible for maintaining 6mA sites within the sequence motif of C**A**GCN($_6$)CTC in *Psph*.

Transcriptomic analysis profiling of differentially regulated genes associated with virulence and metabolism in the HsdMSR mutant

To explore the regulatory influence of HsdMSR on gene expression, RNA-seq was applied to analyse WT and Δ*hsdMSR* in the stationary growth phase, which ensured that the strains had sufficient DNA methylation levels. Differentially expressed genes (DEGs) were obtained with the cut-off of $|\log_2 FC| > 1$ and an adjusted p-value < 0.05. We identified 395 DEGs between WT and Δ*hsdMSR* under these experimental conditions. Among these, 218 genes were upregulated, while 177 genes were downregulated compared with the WT (**Fig. 4A** and Table S3). To investigate the functional differences between WT and Δ*hsdMSR*, GO and KEGG databases were used to perform functional enrichment analyses based on the DEGs. When using adjusted p-value < 0.05 as a significant cut-off, the upregulated functional terms included alginate biosynthesis, fructose and

mannose metabolism, and the oxidation– reduction process (**Fig. 4B**). The downregulated pathways included the citrate cycle, oxidative phosphorylation, ribosome structure, and translation (**Fig. 4B**). A total of 116 genes with bigger differences ($|Log_2FC| > 2$) except for genes related to ribosomal protein, T3SS, and alginate synthesis. Among these genes, 31 were annotated as hypothetical proteins and 4 as transcription factors with unknown functions, and the remaining genes mostly encoded metabolism-related enzymes. These enzymes might have effects on growth defects in Δ*hsdMSR*.

We also analysed the function alteration via COG category analysis of DEGs, which revealed that the upregulated genes were more likely to be involved in lanes E (amino acid transport and metabolism), G (carbohydrate transport and metabolism), and I (lipid transport and metabolism) (**Fig. 4C**). Downregulated DEGs were significantly involved in lanes F (nucleotide transport and metabolism) and J (translation, ribosomal structure, and biogenesis) (**Fig. 4D**). To investigate the correlation between DEGs and HsdM-recognising motif sites, we performed comparative analysis. Although the overlap was not statistically significant ($p > 0.05$), we identified 76 overlapping genes (**Fig. 4E**). Eight DEGs harboured the HsdMSR methylation motif at the putative promoter region (within 100-bp upstream of the gene) (Table S4).

HsdMSR was required for T3SS and biofilm formation in *P. syringae*

To confirm the RNA-seq results, we performed quantitative real-time PCR (RT-qPCR) experiments on T3SS genes. Several T3SS effector genes were identified as upregulated, including *hopAE1*, *hrpF*, *hrpA2*, *hrpK1*, and *hrpW1*. RT-qPCR was applied under the same conditions as RNA-seq, and the transcriptional levels of all genes were confirmed as being significantly higher in the Δ*hsdMSR* than the WT (**Fig. 5A**). These gene expression levels were restored in the complemented strain. To determine whether the loss of HsdMSR affected the *Psph* virulence phenotypes because of alterations to T3 effectors, we allowed the WT, Δ*hsdMSR*, and complemented strains to infiltrate the primary leaves of bean plants. At 6 days post-inoculation, Δ*hsdMSR* was observed to induce more severe symptoms than the WT and complemented strains (**Fig. 5B**). Overall, HsdMSR inhibited the expression of T3 effectors under KB conditions, and the loss of this modification system enhanced the pathogenicity of the strain during plant infection.

Besides T3SS, alginate biosynthesis-related genes were also observed among the DEGs between WT and Δ*hsdMSR*. Alginate biosynthesis proteins have been demonstrated to be essential for Extracellular polymeric substances (EPS) production, which enhances biofilm formation during the bacterial infection process (47, 48). RT-qPCR experiments were performed on the relevant genes, including *alg8*, *algE*, *alg44*, *algF*, and *algD*. The expression levels of these genes in Δ*hsdMSR* were significantly increased compared with the WT and complemented strain (**Fig. 5C**). To further investigate the influence of HsdMSR on biofilm formation, we performed a crystal violet staining assay to detect biofilm production by the three strains. The intensity of crystal violet staining of biofilms formed by the WT and complemented strains was significantly less strong than that of Δ*hsdMSR* cells (**Fig. 5D**), supporting the role of HsdMSR in controlling biofilm formation. We therefore concluded that HsdMSR regulates the virulence of *P. syringae* by tuning its expression of T3SS and alginate biosynthesis genes.

HsdMSR regulated ribosomal protein synthesis and translational efficiency

We noticed that HsdMSR was important for bacterial growth (Fig. S4), while the expression of many ribosomal protein genes was reduced with the deletion of *hsdMSR* (**Fig. 5E**). Regulation of ribosomal gene expression is essential to the integrity of the ribosome structure, which affects translation (49). Therefore, we hypothesised that the low expression level of ribosome proteins in Δ*hsdMSR* would result in delayed growth. We selected four genes encoding different ribosome subunits (*rplS*, *rpmD*, *rpsS*, and *rpsJ*) to verify the RNA-seq results through RT-qPCR. While *rplS* and *rpmD* encode 50S ribosomal proteins (L19 and L30), *rpsS* and *rpsJ* are responsible for 30S

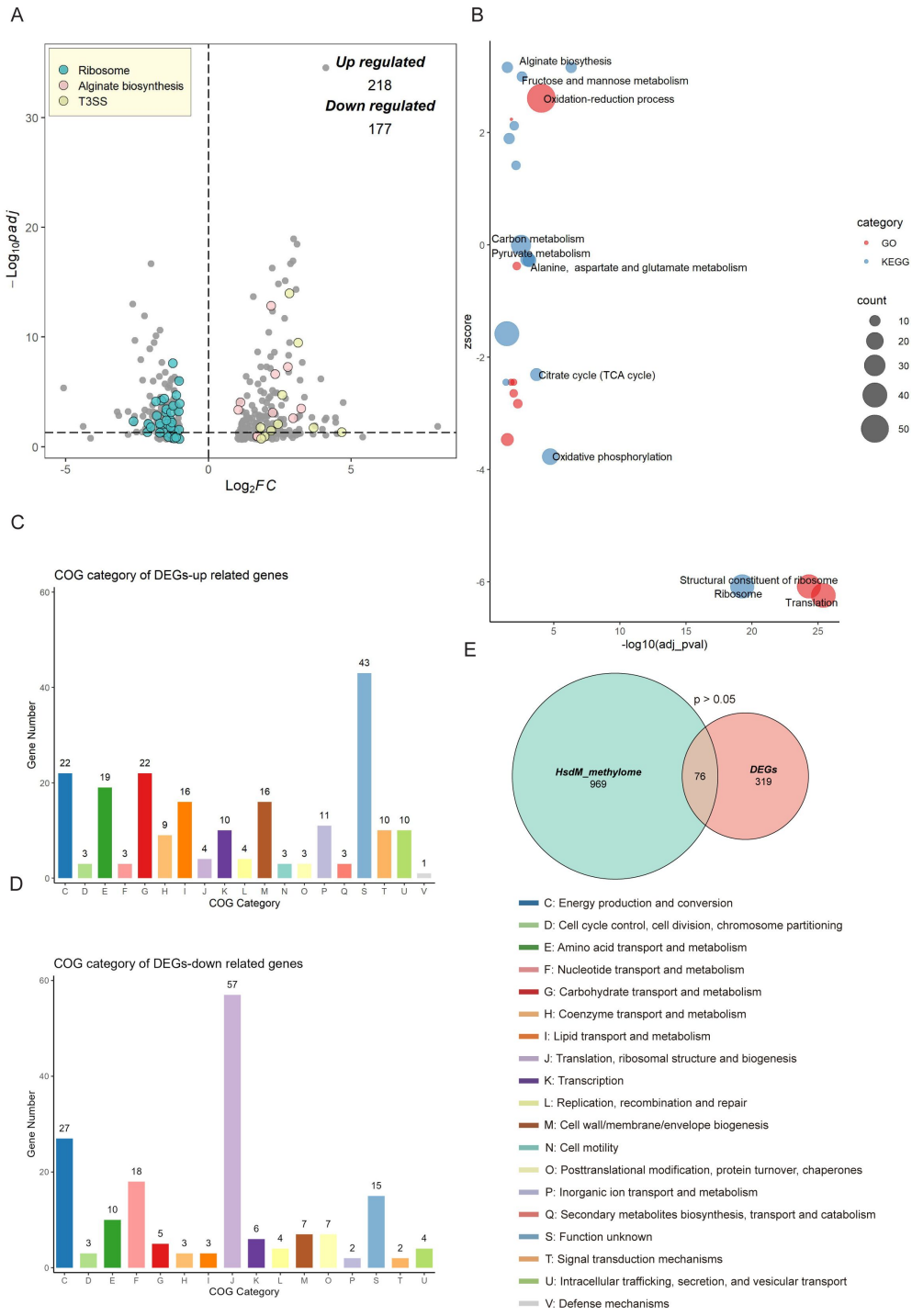

Figure 4.

Transcriptional changes profiling of *hsdMSR* mutant in *Psph*.

(A) The volcano plot reveals DEGs between *Psph* WT and Δ*hsdMSR*. The DEGs were (|$\log_2$ FC| > 1 and adjusted *P* value[<[0.05) in blue (Ribosomal protein), pink (Alginate biosynthesis), and yellow (T3SS). Each dot represents one gene. **(B)** Bubble plot shows enriched GO (Red) and KEGG (Blue) terms based on the DEGs between *Psph* WT and Δ*hsdMSR*. The x-axis shows the significance of functional annotation terms (–log10 adjusted *P*-value), and the y-axis indicates the Z-score of terms. The bubble size represents the gene number of terms. **(C)** COG classification and distribution of up-regulated DEGs. **(D)** COG classification and distribution of down-regulated DEGs. COG terms are highlighted in different colors. **(E)** Venn plot reveals the overlapped genes between DEGs and genes within the HsdMSR motif.

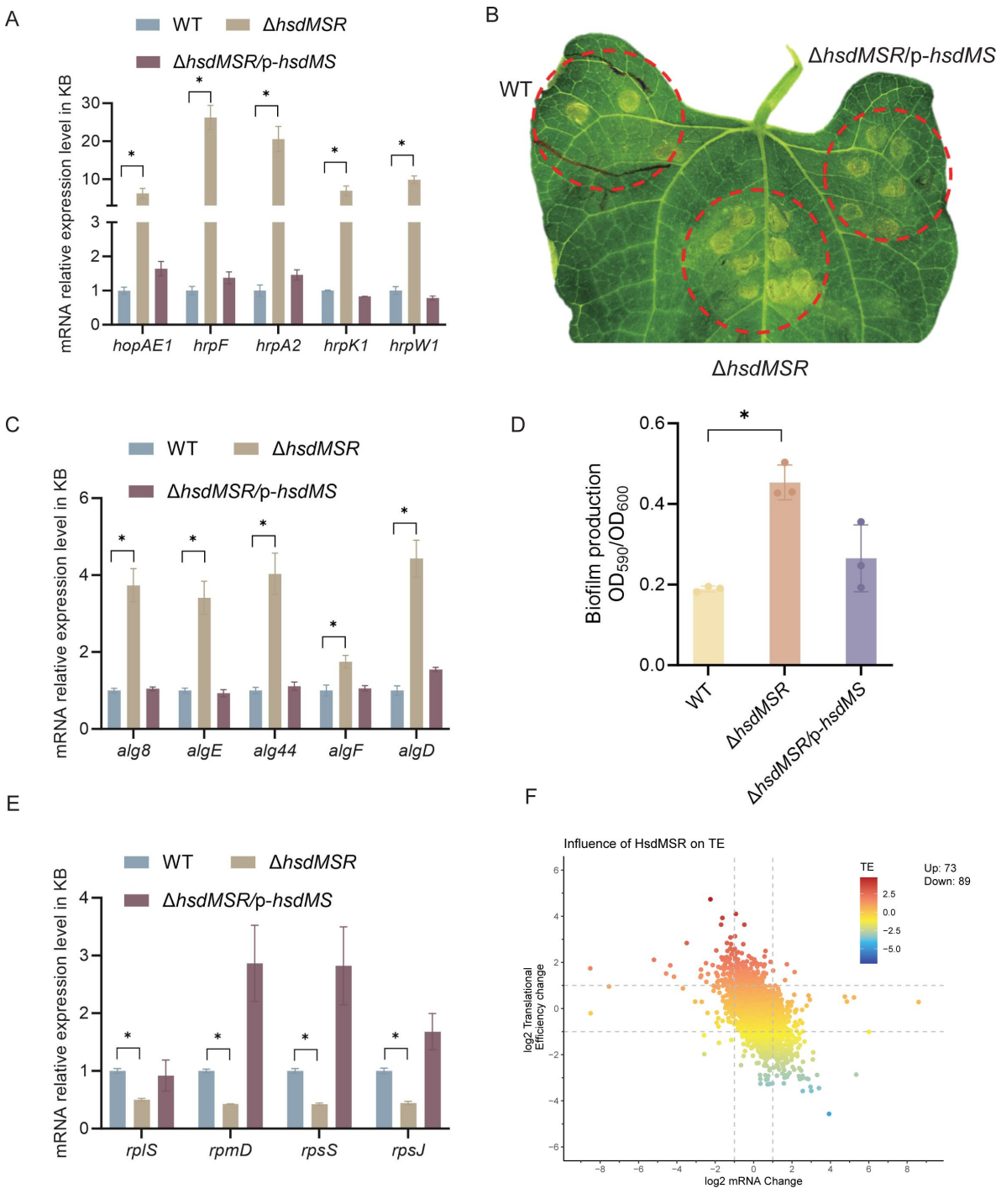

Figure 5.

Influence of HsdMSR on virulence and metabolism in *Psph*.

(A) HsdMSR negatively regulated T3SS-related genes. Data are shown as means ± SD (n = 3). **(B)** Disease symptoms caused by *Psph* WT, Δ*hsdMSR*, and the complemented strains, photographing 6 days after inoculation of 10^5 CFU/mL bacteria. **(C)** HsdMSR negatively regulated alginate biosynthesis-related genes. Data are shown as means ± SD (n = 3). **(D)** The quantification of biofilm production in the *Psph* WT, Δ*hsdMSR*, and the complemented strains using a crystal violate staining assay. **(E)** HsdMSR positively regulated ribosomal protein-related genes. Data are shown as means ± SD (n = 3). **(F)** The scatterplot shows the TE and mRNA change between *Psph* WT and Δ*hsdMSR*. The x-axis presents the log2FC of the mRNA level, and the y-axis shows the $\log_2$FC of the TE. The greater TE is represented in red, whereas the lesser TE is displayed in blue.

ribosomal proteins (S19 and S10). The RT-qPCR results demonstrated that the mRNA expression levels of these genes were significantly lower in Δ*hsdMSR* than in WT, while levels in the complemented strain were restored to the WT level (**Fig. 5E**).

Given the important role of ribosomal proteins in translation, we performed ribosome profiling, also termed Ribo-seq, of the *Psph* WT and Δ*hsdMSR* strains to detect the influence of HsdMSR on translational efficiency (TE). When we compared the WT and Δ*hsdMSR*, the TE of 162 genes was significantly different ($|\log_2 FC| > 1.5$) (**Fig. 5F**). Of these genes, 73 genes had enhanced TE, while 89 had suppressed TE (**Fig. 5F**). Most of these genes were related to transmembrane transport and transcription regulation (Fig. S6A-B). Remarkably, the TE of genes linked to the oxidation-reduction process tended to be suppressed (Fig. S6B). These results showed that HsdMSR plays an important role in the regulation of metabolism by promoting ribosomal protein synthesis and modulating TE in *Psph*.

HsdMSR regulation of *hrpF* was dependent on the full methylation of both strands

To investigate whether and how HsdMSR directly affects gene expression, we focused on those DEGs whose upstream regions harbour its motif. Interestingly, we noticed a methylation motif in the upstream region of *hrpF* (encoding the pathogenicity factor HrpF), which increased its expression level in the *Psph* WT strain (**Fig. 5A** and **6A**). To further explore the effects of HsdMSR on the transcription of *hrpF*, we constructed a *lux*-reporter plasmid carrying the motif and extended it by 50 bp, which covered the upstream region of *hrpF*. After transferring the plasmid into the WT and Δ*hsdMSR* strains, we detected a significant difference in the expression level of *hrpF-lux* between these two strains. The *hrpF-lux* signal in Δ*hsdMSR* increased along with culture time and reached a peak at 24 hours when the methylation level was also elevated in the late growth stage (**Fig. 6B**). This result of the *lux*-reporter assay confirmed the RNA-seq and RT-qPCR results showing that *hrpF* was remarkably upregulated in Δ*hsdMSR* compared with the WT strain.

To detect the influence of the 6mA site within the HsdMSR motif on the expression of *hrpF*, we induced a point mutation on the single strand in the reporter plasmid to change the 6mA to C (C**C**GCN$_6$CTC/ CCGCN$_6$C**G**C). This resulted in a low *hrpF* expression level similar to that of the WT sequence carrying the A base (**Fig. 6C**), indicating that a hemi-methylated pattern is insufficient for transcriptional alteration. To verify our hypothesis, we constructed a reporter with two A mutations (C**C**GCN$_6$C**G**C), transferred it to the WT and Δ*hsdMSR* strains, and detected signal changes. As expected, the reporter carrying the HsdMSR motif without two A bases resulted in a significantly higher signal than the hemi-mutated and non-mutated reporters in the WT (**Fig. 6C**). Taken together, the results showed that HsdMSR regulation of *hrpF* transcription was based on both strands being fully methylated.

Discussion

Recent advances in sequencing technology have expanded our understanding of DNA methylation in bacteria. Numerous DNA MTases have been extensively characterised in different pathogenic bacteria, and data on their distribution patterns, recognition motifs, and biological functions have been collated (31, 32, 50–53). However, most research has concentrated on animal pathogenic bacteria, with limited insights into phytopathogenic bacteria except for *Xanthomonas*(54–56). Consequently, in this study, we employed SMRT-seq to profile the methylome patterns and specific conserved sequence motifs of three *P. syringae* strains. Notably, we discovered that the virulence and metabolism of *Psph* are regulated by Type I R-M MTase HsdM. The nonfunctional nature of the subunit restriction endonuclease HsdR was acknowledged, although its potential functionality relies on the presence of MTase (30).

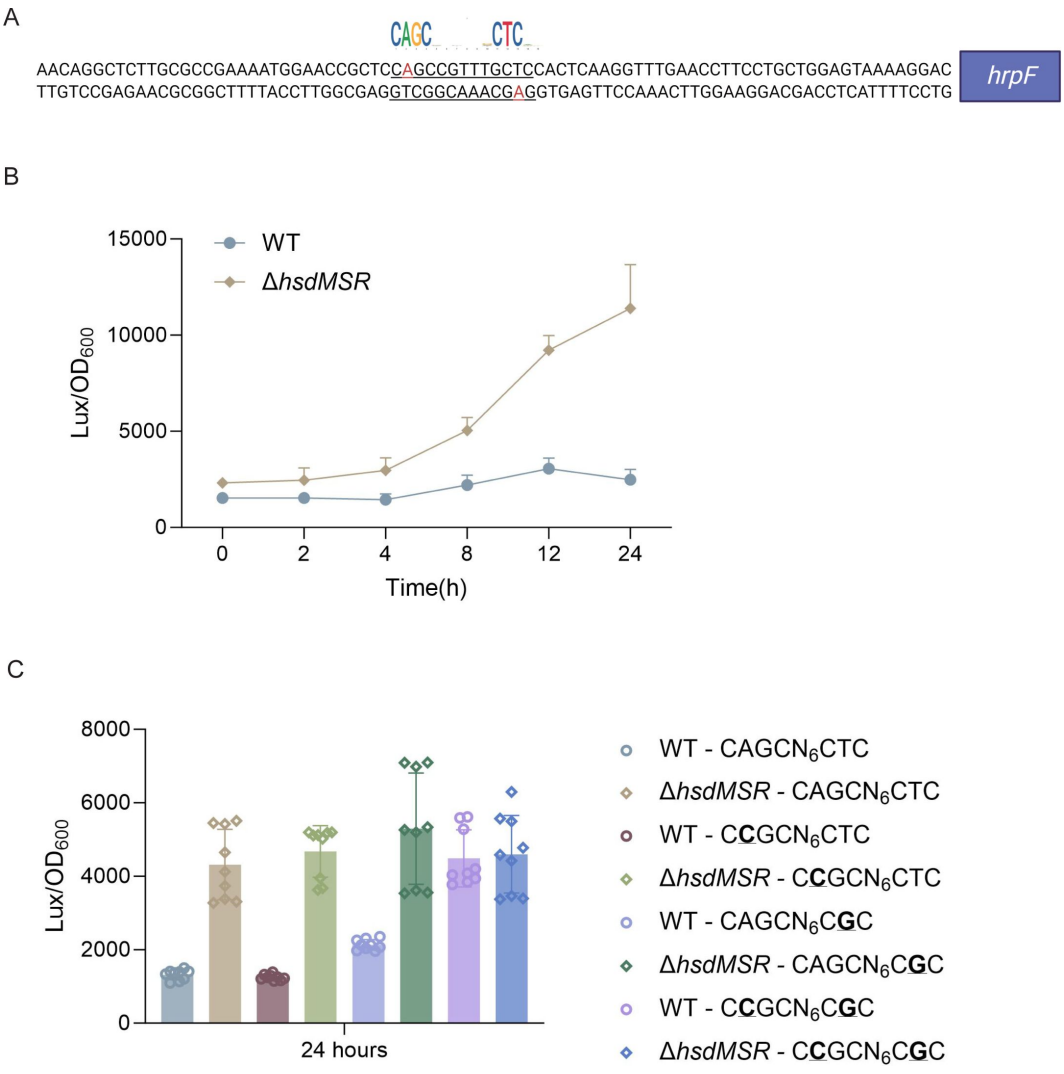

Figure 6.

6mA methylation regulates gene transcription based on fully methylated.

(A) Upstream region sequence of *hrpF* carrying the HsdMSR motif. Adenine methylation is highlighted in red. **(B)** Constantly lux activity detection of the *hrpF* between *Psph* WT and Δ*hsdMSR*. **(C)** Lux activity of *hrpF* between *Psph* WT and Δ*hsdMSR* with single- or double-point mutations. In the HsdMSR motif, "A" was replaced by "C" or "T" was replaced by "G", highlighted in bold and underlined.

Comprehensive analysis of the methylome atlas revealed that 6mA is the most prevalent modification type in *Psph* and *Pst*, mirroring the trends observed in other bacteria. Conversely, *Pss* displays the lowest occurrences of 6mA throughout its genome (**Fig. 1**). This discrepancy might be attributed to the absence of the Type I R-M MTase responsible for 6mA in *Pss*. Similarly, the presence of two Type I R-M MTases in *Pst* possibly contribute to it having a higher number of 6mA sites than *Psph*. Additionally, all three pathovars had a similar pattern, with 4mC being the least frequent modification type. Despite belonging to the same *P. syringae* species, the three strains tested displayed remarkably divergent methylation patterns, which is reminiscent of the phenomenon observed in *Xanthomonas* spp. (54).

We further identified two (both 6mA) and four (three 6mA, one 4mC) motifs in *Psph* and *Pst*, respectively, but none in *Pss* (**Fig. 3**). In fact, more motifs were predicted by the MEME and PacBio motif finders, but we chose only those motifs identified by both algorithms for higher accuracy. We found that the 6mA motifs had extremely high methylation levels, ranging from 77% to 100%, in the stationary phase of *P. syringae*. We subsequently found that the 6mA methylation levels increased during *Psph* growth, similar to the observations in *P. aeruginosa* (30). However, DNA methylation is much more stable under different conditions and growth phases in *Helicobacter pylori* and *Salmonella typhimurium* (57, 58).

MTases have been reported to play important roles in bacterial growth; for example, they are involved in cell cycle processes such as chromosomal replication in *E. coli* and *Caulobacter crescentus* (59–61). DNA methylation can activate DnaA and signal the initiation of chromosome replication to affect the growth of gamma-proteobacteria (62, 63). Previous studies revealed that DNA methylation influences bacterial growth through genes related to diverse carbohydrate transport mechanisms (55). We report that the 6mA modification catalysed by HsdM in *Psph* positively affects its growth, which can be explained by the downregulation of ribosomal proteins and the alteration of metabolism-related gene TE. However, many MTases are thought to be uncorrelated to growth in bacterial species such as *P. aeruginosa* and *Klebsiella pneumoniae* (30, 31, 52).

Many MTases and DNA methylations are involved in bacterial virulence through their modulation of gene expression (30, 31, 52, 53, 55, 56, 64–66). In this study, RNA-seq analysis of the HsdMSR mutation strain revealed 395 DEGs. Remarkably, not all DEGs harboured the HsdMSR methylation motif in their promoter region. There were no significant correlations between the HsdM-recognised motif sites in the promoter region and DEGs, even though DNA methylation is generally known to affect gene expression by altering the interactions between DNA and proteins such as TFs, which compete with MTases at specific motif sites and thus influence downstream transcription (67). However, recent studies have revealed that DNA methylation within CDS can also alter gene expression in bacteria; for example, 5mC in CDS can enhance transcription while blocking the transcription of CpG islands in promoters in eukaryotic cells (68, 69). We hypothesise that 6mA in *Psph* can regulate gene expression directly and indirectly. We confirmed that the 6mA motif in the promoter region of *hrpF* can directly and negatively regulate gene transcription in a manner dependent on full methylation of the strands (**Fig. 6**). In addition, DNA methylation can change DNA curvature to decrease the thermodynamic stability of the double helix (70). Therefore, those DEGs carrying modified sites, including alginate biosynthesis-related genes and T3 effectors, are believed to be caused by the alteration of nucleoid topology, as seen in *Salmonella* and *H. pylori* (53, 71). Furthermore, the 6mA sites, including those in virulence-related *hrc/hrp* and *alg* genes, are conserved in *Psph* and *Pst*, implying that similar phenotypes occur in the latter strain. Altogether, 6mA modifications in *Psph* were observed to act as important epigenetic regulators of gene expression.

Apart from the established roles of 6mA and HsdMSR in *P. syringae*, certain signals or factors may influence HsdMSR expression. For instance, we confirmed that the growth phase affects methylation levels in *P. syringae*. Previous studies have shown that increased temperatures can

reduce methylation levels, as observed in PAO1 (30). These findings suggest that HsdMSR expression may be responsive to both intrinsic cellular states and extrinsic environmental conditions. To further explore potential upstream TFs regulating the expression of HsdMSR, we searched for TF-binding sites in the HsdMSR promoter using our own databases (16, 18, 72). As a result, we found three candidate TFs (PSPPH_0061, PSPPH_3268, and PSPPH_3504) that might directly bind and regulate HsdMSR expression. Future studies on these TFs and their interactions with the HsdMSR promoter would help clarify the regulatory network governing HsdMSR activity.

Moreover, RM systems are known for their intrinsic role as innate immune systems in anti-phage infection, and present in around 90% of bacterial genomes (73). RM systems protect bacteria self by recognizing and degrading foreign phage DNA via methylation-specific site and restriction endonucleases (REases) (74). In addition, other phage-resistance systems are similar to RM systems but carry extra genes. One is called the phage growth limitation (Pgl) system, which modifies and cleaves phage DNA. However, the Pgl only modifies the phage DNA in the first infection cycle, and cleaves phage DNA in the subsequent infections, which gives a warn to the neighboring cells (75, 76). To counteract RM and RM-like systems, phages have evolved strategies, including unusual modifications such as hydroxymethylation, glycosylation, and glucosylation. They can also encode their own MTases to protect their DNA or employ strategies to evade restriction systems and other anti-RM defenses (77–79).

As more studies apply SMRT-seq to investigate bacterial methylomes, it has become evident that the epigenetic regulation of gene expression is highly prevalent among bacteria. Understanding the mechanisms through which methylation functions can provide novel insights into how strain-specific epigenetic modifications shape the adaptive responses of bacteria to distinct environmental challenges. As the repertoire of MTases varies among *P. syringae* strains, this approach will help us to better understand the diversity of DNA methylation and epigenetic patterns among *P. syringae* species.

Materials and methods

Bacterial strains and culture conditions

The bacterial strains, plasmids, and primers used in this study can be found in Table S5. All three model strains and mutations were cultured at 28[in KB medium with shaking at 220 rpm or LB agar plates. The *E. coli* strains were grown at 37[in LB broth (Luria-Bertani) with shaking at 220 rpm or on LB agar plates. Antibiotics were used at the following concentrations: kanamycin at 50 μg/mL, spectinomycin at 50 μg/mL, and rifampin 25 μg/mL.

DNA extraction and SMRT sequencing

Three WT model strains and HsdMSR knockout *Psph* strains were cultured to the stationary phase. The genomic DNA of the strains was extracted using a TIANamp Bacteria DNA kit (Tiangen Biotech), using the manufacturer's standard protocols. The SMRT sequence was performed at Abace Biotechnology company using Pacific Biosciences sequel II and Ile sequencer (PacBio, Menlo Park, CA, USA). SMRT-seq reads were aligned to the genome reference of *Psph* 1448A (GCF_000012205.1), *Pst* DC3000 (GCF_000007805.1), and *Pss* B728a (GCF_000012245.1), respectively. SMRTLink software v13.0 was used to perform DNA methylation analysis. A modification quality value (QV) score of 50 and 100 was used to call the modified bases A and C, respectively.

Deletion mutant and complemented strains construction

The restriction enzymes digested the pK18mobsacB suicide plasmid (80) listed in Table S5. The upstream (~1500-bp) and downstream (~1000-bp) fragments of HsdMSR open reading frame (ORF) were amplified from the *Psph* genome and digested. Then, the digested upstream and downstream fragments were ligated with T4 DNA ligase (NEB). The ligated fragments were inserted into the digested plasmid using ClonExpress MultiS One Step Cloning Kit (Vazyme). The recombinant plasmids were transformed into the *Psph* WT strain in the KB plate with rifampin and kanamycin. The single colonies were picked to a sucrose plate and then cultured in both KB with kanamycin/rifampin and KB with rifampin alone. Loss of kanamycin resistance indicated a double crossover. Finally, the deletion strains were further confirmed by qRT-PCR to detect the mRNA level of HsdMSR. For the complemented plasmids, the ORF of HsdMS was amplified by PCR from the *Psph* genome and cloned into the pHM1 plasmid.

Growth curve measure assay

Overnight cultures of *Psph* and Δ*hsdMSR* were diluted to an OD_{600} of 0.1 in fresh KB liquid medium for use as the inoculum. One hundred μL of the inoculum was aliquoted into a 96-well microtiter plate in triplicate and incubated at 28°C for growth. OD_{600} values were recorded per 2 h for 8 times for plotting of growth curves.

Dot blotting assay

Dot blotting was performed as previously described (81). Briefly, DNA samples were denatured at 95°C for 10 minutes and cooled down on ice for 3 minutes. Samples were spotted on the nylon membrane and air dry for 5 minutes, followed by heat-crosslink at 80[for 2 hours. Membranes were blocked in 5% nonfat dry milk in TBST for 1 hour at room temperature, incubated with N^6-mA antibodies (1:1000) overnight at 4°C. After 5 washes with TBST, membranes were incubated with HRP-linked secondary anti-rabbit IgG antibody (1:5,000) for 1 hour at room temperature. Signals were detected with ChemiDoc Imaging Systems (Bio-Rad). After imaging, incubate the membrane with methylene blue staining buffer for 15 minutes with gentle shaking.

RNA-seq analyses

Psph and Δ*hsdMSR* strains were first cultured to the stationary phase in KB medium at 28°C. Cultures were collected, and total RNA was extracted using the RNeasy mini kit (Qiagen) following the manufacturer's protocol and genomic DNA contamination was removed by DNaseI treatment (NEB). Subsequently, rRNA was depleted by using the MICROBExpress kit (Ambion), and the remaining mRNA was used to generate the cDNA library according to the NEBNext® UltraTM II RNA Library Prep Kit protocol (Illumina), which was then sequenced using the Illumina HiSeq 2000 system, generating 150-bp paired-end reads. Two biological replications have been performed. For each RNA-seq sample, raw sequencing reads were quality-trimmed using trim_galore (version 0.6.7) and aligned to the *Psph* genome using hisat2 (version 7.5.0)(82). DEGs were identified using DESeq2(83), and Function enrichment analysis of DEGs was conducted using the R package clusterProfiler(84).

Ribo-seq library construction and analysis

The construction of the Ribo-seq library followed the previous protocol(85). Briefly, bacteria were cultured to an OD_{600} of 0.4, at which point chloramphenicol was added to a final concentration of 100 μg/mL for 2 minutes. Cells were then pelleted and washed with pre-chilled lysis buffer [25 mM Tris-HCl, pH 8.0; 25 mM NH_4Cl; 10 mM MgOAc; 0.8% Triton X-100; 100 U/mL RNase-free DNase I; 0.3 U/mL Superase-In; 1.55 mM chloramphenicol; and 17 mM GMPPNP]. The pellet was resuspended in lysis buffer, followed by three freeze-thaw cycles using liquid nitrogen. Sodium deoxycholate was then added to a final concentration of 0.3% before centrifugation. The

resulting supernatant was adjusted to 25 A_{260} units and mixed with 2 mL of 500 mM $CaCl_2$ and 12 µL MNase, making up a total volume of 200 µL. After the digestion, the reaction was quenched with 2.5 mL of 500 mM EGTA. Monosomes were isolated using Sephacryl S400 MicroSpin columns, and RNA was purified using the miRNeasy Mini Kit (Qiagen). rRNA was removed using the NEBNext rRNA Depletion Kit, and the final library was constructed with the NEBNext Small RNA Library Prep Kit. For each sample, ribosome footprint reads were mapped to the *Psph* 1448A reference genome, and the translational efficiency was calculated by dividing the normalized Ribo-seq counts by the normalized RNA counts. Two biological replicates were performed for all experiments.

Real-time quantitative PCR (RT-qPCR) verification

For RT-qPCR, RNA was purified using the RNeasy minikit (Qiagen). The cDNA synthesis was performed using a FastKing RT Kit (Tiangen Biotech). The assay was performed by SuperReal Premix Plus (SYBR Green) Kit (Tiangen Biotech) according to the manufacturer's instruction. Each sample was repeated thrice with 600 ng cDNA and 16S rRNA as the internal control. The fold change represents the relative expression level of mRNA, which can be estimated by the threshold cycle (Ct) values of $2^{-(\Delta\Delta Ct)}$.

Plant infection assay

The bean (*Phaseolus vulgaris* cv. *Red Kidney*) plants were used for the pathogenicity assay. The plant was grown in a greenhouse, as described previously (86). Overnight bacterial cultures were diluted to OD600 = 0.2×10^{-3} and were hand-inoculated into the primary leaves of week-old bean plants for 6 days.

Biofilm formation assay

Biofilm production was detected, as previously reported (87). In brief, overnight bacterial cultures of *Psph* WT and HsdMSR mutants were diluted into OD600 = 0.1 and transferred to a 10 ml borosilicate tube containing 1 ml KB medium. Then, the cultures grow statically at 28°C for 3-5 days. Then, 0.1% crystal violet was used to stain the biofilm adhered to the tube tightly for 30 min, and other components bound to the tube loosely were washed off with distilled deionized water. The remaining crystal violet was fully dissolved in 1 ml 95%~100% ethanol with constant shaking. Then, it was transferred to a transparent 96-well plate to measure its optical density at 590 nm using a Biotech microplate reader. The experiment was repeated using three independent bacterial cultures.

Data analysis and statistics

The graphs in this paper were plotted using ggplot2 in R 4.2.0 software and GraphPad Prism 10.0.3 (GraphPad Inc.) Differences between groups were analyzed using students' two-tailed t-tests. The results of all statistical analyses are shown as mean ± standard deviation (SD). All experiments were repeated independently at least three times with similar results.

Data availability

The Ribo-seq, RNA-seq data, and SMRT-seq data were uploaded to the National Center for Biotechnology Information SRA database as part of BioProject PRJNA1055550 and PRJNA1123379, respectively. Codes were available upon reasonable request.

Acknowledgements

This study was supported by grants from Guangdong Major Project of Basic and Applied Basic Research (2020B0301030005), Shenzhen Science and Technology Fund (JCYJ20210324134000002), the National Natural Science Foundation of China (32172358), General Research Funds of Hong Kong (11103221, 11101722, 11102223), the Sichuan Province Science and Technology Planning Project (2021YFSY0005). The funders had no role in study design, data collection, interpretation, or the decision to submit the work for publication.

Additional information

Author contribution

Conceptualization, J.H., and X.D; Methodology, J.H.; Validation, J.H., F.C., B.L., Y.Y., and Y.S.; Investigation, J.H., F.C. and B.L.; Writing & Editing, J.H., and X.D; Supervision X.D

References

1. Bull CT, De Boer SH, Denny TP, Firrao G, Saux MF-L, Saddler GS, Scortichini M, Stead DE, Takikawa Y. 2010) **Comprehensive list of names of plant pathogenic bacteria, 1980-2007** *Journal of Plant Pathology* :551–592

2. Xin X-F, Kvitko B, He SY 2018) **Pseudomonas syringae: what it takes to be a pathogen** *Nature Reviews Microbiology* **16**:316–328

3. Arnold DL, Lovell HC, Jackson RW, Mansfield JW 2011) **Pseudomonas syringae pv. phaseolicola: from 'has bean' to supermodel** *Molecular Plant Pathology* **12**:617–627

4. Xin XF, He SY 2013) **Pseudomonas syringae pv. tomato DC3000: a model pathogen for probing disease susceptibility and hormone signaling in plants** *Annu Rev Phytopathol* **51**:473–98

5. Monier JM, Lindow SE 2005) **Aggregates of resident bacteria facilitate survival of immigrant bacteria on leaf surfaces** *Microb Ecol* **49**:343–52

6. Clarke CR, Cai R, Studholme DJ, Guttman DS, Vinatzer BA 2010) **Pseudomonas syringae strains naturally lacking the classical P. syringae hrp/hrc Locus are common leaf colonizers equipped with an atypical type III secretion system** *Mol Plant Microbe Interact* **23**:198–210

7. Rahme LG, Mindrinos MN, Panopoulos NJ 1992) **Plant and environmental sensory signals control the expression of hrp genes in Pseudomonas syringae pv. phaseolicola** *J Bacteriol* **174**:3499–507

8. Xiao F, Goodwin SM, Xiao Y, Sun Z, Baker D, Tang X, Jenks MA, Zhou JM 2004) **Arabidopsis CYP86A2 represses Pseudomonas syringae type III genes and is required for cuticle development** *EMBO J* **23**:2903–13

9. Xiao Y, Lu Y, Heu S, Hutcheson SW 1992) **Organization and environmental regulation of the Pseudomonas syringae pv. syringae 61 hrp cluster** *J Bacteriol* **174**:1734–41

10. Xiao Y, Heu S, Yi J, Lu Y, Hutcheson SW 1994) **Identification of a putative alternate sigma factor and characterization of a multicomponent regulatory cascade controlling the expression of Pseudomonas syringae pv. syringae Pss61 hrp and hrmA genes** *J Bacteriol* **176**:1025–36

11. Hutcheson SW, Bretz J, Sussan T, Jin S, Pak K 2001) **Enhancer-binding proteins HrpR and HrpS interact to regulate hrp-encoded type III protein secretion in Pseudomonas syringae strains** *J Bacteriol* **183**:5589–98

12. Hendrickson EL, Guevera P, Ausubel FM 2000) **The alternative sigma factor RpoN is required for hrp activity in Pseudomonas syringae pv. maculicola and acts at the level of hrpL transcription** *Journal of bacteriology* **182**:3508–3516

13. Haefele DM, Lindow SE 1987) **Flagellar motility confers epiphytic fitness advantages upon Pseudomonas syringae** *Applied and Environmental Microbiology* **53**:2528–2533

14. Dasgupta N, Wolfgang MC, Goodman AL, Arora SK, Jyot J, Lory S, Ramphal R 2003) **A four-tiered transcriptional regulatory circuit controls flagellar biogenesis in Pseudomonas aeruginosa pv. tomato DC3000** *Mol Microbiol* **50**:809–24

15. Deng X, Liang H, Chen K, He C, Lan L, Tang X 2014) **Molecular mechanisms of two-component system RhpRS regulating type III secretion system in Pseudomonas syringae** *Nucleic Acids Res* **42**:11472–86

16. Fan L, Wang T, Hua C, Sun W, Li X, Grunwald L, Liu J, Wu N, Shao X, Yin Y, Yan J, Deng X 2020) **A compendium of DNA-binding specificities of transcription factors in Pseudomonas syringae** *Nat Commun* **11**

17. Xie Y, Ding Y, Shao X, Yao C, Li J, Liu J, Deng X 2021) **Pseudomonas syringae senses polyphenols via phosphorelay crosstalk to inhibit virulence** *EMBO Rep* **22**

18. Shao X, Tan M, Xie Y, Yao C, Wang T, Huang H, Zhang Y, Ding Y, Liu J, Han L, Hua C, Wang X, Deng X 2021) **Integrated regulatory network in Pseudomonas syringae reveals dynamics of virulence** *Cell Rep* **34**

19. Huang J, Yao C, Sun Y, Ji Q, Deng X 2022) **Virulence-related regulatory network of Pseudomonas syringae** *Comput Struct Biotechnol J* **20**:6259–6270

20. Gold M, Hurwitz J, Anders M 1963) **The enzymatic methylation of RNA and DNA. II. On the species specificity of the methylation enzymes** *Proceedings of the National Academy of Sciences* **50**:164–169

21. Casadesus J, Low D 2006) **Epigenetic gene regulation in the bacterial world** *Microbiol Mol Biol Rev* **70**:830–56

22. Wion D, Casadesus J 2006) **N6-methyl-adenine: an epigenetic signal for DNA-protein interactions** *Nat Rev Microbiol* **4**:183–92

23. Bickle TA, Kruger DH 1993) **Biology of DNA restriction** *Microbiol Rev* **57**:434–50

24. Loenen WA, Dryden DT, Raleigh EA, Wilson GG 2014) **Type I restriction enzymes and their relatives** *Nucleic Acids Res* **42**:20–44

25. Blow MJ, Clark TA, Daum CG, Deutschbauer AM, Fomenkov A, Fries R, Froula J, Kang DD, Malmstrom RR, Morgan RD, Posfai J, Singh K, Visel A, Wetmore K, Zhao Z, Rubin EM, Korlach J, Pennacchio LA, Roberts RJ 2016) **The Epigenomic Landscape of Prokaryotes** *PLoS Genet* **12**

26. Beaulaurier J, Schadt EE, Fang G 2019) **Deciphering bacterial epigenomes using modern sequencing technologies** *Nat Rev Genet* **20**:157–172

27. Ho J, Taiaroa G, Butler MI, Poulter RTM 2019) **The Genome Sequence of M228, a Chinese Isolate of Pseudomonas syringae pv. actinidiae** *Illustrates Insertion Sequence Element Mobility. Microbiol Resour Announc* **8**

28. Poulter RTM, Ho J, Handley T, Taiaroa G, Butler MI. 2018) **Scientific Reports**

29. Poulter R, Taiaroa G, Sumpter N, Stockwell P, Butler M 2017) **Complete Genome Sequence of the Kiwifruit Pathogen Pseudomonas syringae pv. actinidiae Biovar 5, Originating from Japan** *Genome Announc* **5**

30. Doberenz S, Eckweiler D, Reichert O, Jensen V, Bunk B, Sproer C, Kordes A, Frangipani E, Luong K, Korlach J, Heeb S, Overmann J, Kaever V, Haussler S 2017) **Identification of a Pseudomonas aeruginosa PAO1 DNA Methyltransferase, Its Targets, and Physiological Roles** *mBio* **8**

31. Han S, Liu J, Li M, Zhang Y, Duan X, Zhang Y, Chen H, Cai Z, Yang L, Liu Y 2022) **DNA Methyltransferase Regulates Nitric Oxide Homeostasis and Virulence in a Chronically Adapted Pseudomonas aeruginosa Strain** *mSystems* **7**

32. Li Z, Zhou X, Liao D, Liu R, Zhao X, Wang J, Zhong Q, Zeng Z, Peng Y, Tan Y, Yang Z 2023) **Comparative genomics and DNA methylation analysis of Pseudomonas aeruginosa clinical isolate PA3 by single-molecule real-time sequencing reveals new targets for antimicrobials** *Front Cell Infect Microbiol* **13**

33. Roberts RJ, Vincze T, Posfai J, Macelis D 2023) **REBASE: a database for DNA restriction and modification: enzymes, genes and genomes** *Nucleic Acids Res* **51**:D629–D630

34. Bird A 2002) **DNA methylation patterns and epigenetic memory** *Genes & development* **16**:6–21

35. Gelfman S, Cohen N, Yearim A, Ast G 2013) **DNA-methylation effect on cotranscriptional splicing is dependent on GC architecture of the exon–intron structure** *Genome research* **23**:789–799

36. Militello KT, Simon RD, Qureshi M, Maines R, Van Horne ML, Hennick SM, Jayakar SK, Pounder S. 2012) **Conservation of Dcm-mediated cytosine DNA methylation in Escherichia coli** *FEMS microbiology letters* **328**:78–85

37. Nur I, Szyf M, Razin A, Glaser G, Rottem S, Razin S 1985) **Procaryotic and eucaryotic traits of DNA methylation in spiroplasmas (mycoplasmas)** *Journal of bacteriology* **164**:19–24

38. Jin M, Chen J, Zhao X, Hu G, Wang H, Liu Z, Chen W-H 2022) **An engineered λ phage enables enhanced and strain-specific killing of enterohemorrhagic Escherichia coli** *Microbiology Spectrum* **10**:e01271–22

39. Ashburner M, Ball CA, Blake JA, Botstein D, Butler H, Cherry JM, Davis AP, Dolinski K, Dwight SS, Eppig JT, Harris MA, Hill DP, Issel-Tarver L, Kasarskis A, Lewis S, Matese JC, Richardson JE, Ringwald M, Rubin GM, Sherlock G 2000) **Gene ontology: tool for the unification of biology. The Gene Ontology Consortium** *Nat Genet* **25**:25–9

40. Kanehisa M, Goto S 2000) **KEGG: kyoto encyclopedia of genes and genomes** *Nucleic Acids Res* **28**:27–30

41. Cantalapiedra CP, Hernandez-Plaza A, Letunic I, Bork P, Huerta-Cepas J 2021) **eggNOG-mapper v2: Functional Annotation, Orthology Assignments, and Domain Prediction at the Metagenomic Scale** *Mol Biol Evol* **38**:5825–5829

42. Huerta-Cepas J, Szklarczyk D, Heller D, Hernandez-Plaza A, Forslund SK, Cook H, Mende DR, Letunic I, Rattei T, Jensen LJ, von Mering C, Bork P. 2019) **eggNOG 5.0: a hierarchical, functionally and phylogenetically annotated orthology resource based on 5090 organisms and 2502 viruses** *Nucleic Acids Res* **47**:D309–D314

43. Bailey TL, Johnson J, Grant CE, Noble WS 2015) **The MEME Suite** *Nucleic Acids Res* **43**:W39–49

44. Gonzalez D, Collier J 2013) **DNA methylation by CcrM activates the transcription of two genes required for the division of Caulobacter crescentus** *Mol Microbiol* **88**:203–18

45. Krebes J, Morgan RD, Bunk B, Sproer C, Luong K, Parusel R, Anton BP, Konig C, Josenhans C, Overmann J, Roberts RJ, Korlach J, Suerbaum S 2014) **The complex methylome of the human gastric pathogen Helicobacter pylori** *Nucleic Acids Res* **42**:2415–32

46. Sanchez-Romero MA, Casadesus J 2020) **The bacterial epigenome** *Nat Rev Microbiol* **18**:7–20

47. Boyd A, Chakrabarty A 1995) **Pseudomonas aeruginosa biofilms: role of the alginate exopolysaccharide** *Journal of industrial microbiology and biotechnology* **15**:162–168

48. Ichinose Y, Taguchi F, Mukaihara T 2013) **Pathogenicity and virulence factors of Pseudomonas syringae** *Journal of General Plant Pathology* **79**:285–296

49. Zhou X, Liao WJ, Liao JM, Liao P, Lu H 2015) **Ribosomal proteins: functions beyond the ribosome** *J Mol Cell Biol* **7**:92–104

50. Murray IA, Clark TA, Morgan RD, Boitano M, Anton BP, Luong K, Fomenkov A, Turner SW, Korlach J, Roberts RJ 2012) **The methylomes of six bacteria** *Nucleic Acids Res* **40**:11450–62

51. Lee WC, Anton BP, Wang S, Baybayan P, Singh S, Ashby M, Chua EG, Tay CY, Thirriot F, Loke MF, Goh KL, Marshall BJ, Roberts RJ, Vadivelu J 2015) **The complete methylome of Helicobacter pylori UM032** *BMC Genomics* **16**

52. Fang CT, Yi WC, Shun CT, Tsai SF 2017) **DNA adenine methylation modulates pathogenicity of Klebsiella pneumoniae genotype K1** *J Microbiol Immunol Infect* **50**:471–477

53. Kumar S, Karmakar BC, Nagarajan D, Mukhopadhyay AK, Morgan RD, Rao DN 2018) **N4-cytosine DNA methylation regulates transcription and pathogenesis in Helicobacter pylori** *Nucleic Acids Res* **46**

54. Seong HJ, Park HJ, Hong E, Lee SC, Sul WJ, Han SW 2016) **Methylome Analysis of Two Xanthomonas spp. Using Single-Molecule Real-Time Sequencing** *Plant Pathol J* **32**:500–507

55. Park HJ, Jung B, Lee J, Han SW 2019) **Functional characterization of a putative DNA methyltransferase, EadM, in Xanthomonas axonopodis pv. glycines by proteomic and phenotypic analyses** . *Sci Rep* **9**

56. Park HJ, Seong HJ, Lee J, Heo L, Sul WJ, Han SW 2021) **Two DNA Methyltransferases for Site-Specific 6mA and 5mC DNA Modification in Xanthomonas euvesicatoria** *Front Plant Sci* **12**

57. Krebes J, Morgan RD, Bunk B, Spröer C, Luong K, Parusel R, Anton BP, König C, Josenhans C, Overmann J 2014) **The complex methylome of the human gastric pathogen Helicobacter pylori** *Nucleic acids research* **42**:2415–2432

58. Bourgeois JS, Anderson CE, Wang L, Modliszewski JL, Chen W, Schott BH, Devos N, Ko DC 2022) **Integration of the Salmonella Typhimurium Methylome and Transcriptome Reveals That DNA Methylation and Transcriptional Regulation Are Largely Decoupled under Virulence-Related Conditions** *mBio* **13**

59. Reyes-Lamothe R, Sherratt DJ 2019) **The bacterial cell cycle, chromosome inheritance and cell growth** *Nat Rev Microbiol* **17**:467–478

60. Gonzalez D, Kozdon JB, McAdams HH, Shapiro L, Collier J 2014) **The functions of DNA methylation by CcrM in Caulobacter crescentus: a global approach** *Nucleic Acids Res* **42**:3720–35

61. Kozdon JB, Melfi MD, Luong K, Clark TA, Boitano M, Wang S, Zhou B, Gonzalez D, Collier J, Turner SW, Korlach J, Shapiro L, McAdams HH 2013) **Global methylation state at base-pair resolution of the Caulobacter genome throughout the cell cycle** *Proceedings of the National Academy of Sciences* **110**:E4658–E4667

62. Seong HJ, Han SW, Sul WJ 2021) **Prokaryotic DNA methylation and its functional roles** *J Microbiol* **59**:242–248

63. Boye E, Stokke T, Kleckner N, Skarstad K 1996) **Coordinating DNA replication initiation with cell growth: differential roles for DnaA and SeqA proteins** *Proc Natl Acad Sci U S A* **93**:12206–11

64. Manzer HS, Brunetti T, Doran KS 2023) **Identification of a DNA-cytosine methyltransferase that impacts global transcription to promote group B streptococcal vaginal colonization** *mBio* 0:e02306–23

65. Banas JA, Biswas S, Zhu M 2011) **Effects of DNA methylation on expression of virulence genes in Streptococcus mutans** *Appl Environ Microbiol* **77**:7236–42

66. Oliveira PH, Ribis JW, Garrett EM, Trzilova D, Kim A, Sekulovic O, Mead EA, Pak T, Zhu S, Deikus G 2020) **Epigenomic characterization of Clostridioides difficile finds a conserved DNA methyltransferase that mediates sporulation and pathogenesis** *Nature microbiology* **5**:166–180

67. Lim HN, van Oudenaarden A 2007) **A multistep epigenetic switch enables the stable inheritance of DNA methylation states** *Nat Genet* **39**:269–75

68. Kahramanoglou C, Prieto AI, Khedkar S, Haase B, Gupta A, Benes V, Fraser GM, Luscombe NM, Seshasayee AS 2012) **Genomics of DNA cytosine methylation in Escherichia coli reveals its role in stationary phase transcription** *Nat Commun* **3**

69. Rishi V, Bhattacharya P, Chatterjee R, Rozenberg J, Zhao J, Glass K, Fitzgerald P, Vinson C 2010) **CpG methylation of half-CRE sequences creates C/EBPα binding sites that activate some tissue-specific genes** *Proceedings of the National Academy of Sciences* **107**:20311–20316

70. Diekmann S 1987) **DNA methylation can enhance or induce DNA curvature** *The EMBO journal* **6**:4213–4217

71. Camacho EM, Serna A, Madrid C, Marques S, Fernandez R, de la Cruz F, Juarez A, Casadesus J 2005) **Regulation of finP transcription by DNA adenine methylation in the virulence plasmid of Salmonella enterica** *J Bacteriol* **187**:5691–9

72. Sun Y, Li J, Huang J, Li S, Li Y, Lu B, Deng X 2024) **Architecture of genome-wide transcriptional regulatory network reveals dynamic functions and evolutionary trajectories in Pseudomonas syringae** *bioRxiv*

73. Oliveira PH, Touchon M, Rocha EP 2014) **The interplay of restriction-modification systems with mobile genetic elements and their prokaryotic hosts** *Nucleic acids research* **42**:10618–10631

74. Loenen WA, Dryden DT, Raleigh EA, Wilson GG, Murray NE 2014) **Highlights of the DNA cutters: a short history of the restriction enzymes** *Nucleic acids research* **42**:3–19

75. Hampton HG, Watson BN, Fineran PC 2020) **The arms race between bacteria and their phage foes** *Nature* **577**:327–336

76. Hoskisson PA, Sumby P, Smith MC 2015) **The phage growth limitation system in Streptomyces coelicolor A (3) 2 is a toxin/antitoxin system, comprising enzymes with DNA methyltransferase, protein kinase and ATPase activity** *Virology* **477**:100–109

77. Vasu K, Nagaraja V 2013) **Diverse functions of restriction-modification systems in addition to cellular defense** *Microbiol Mol Biol Rev* **77**:53–72

78. Murphy J, Mahony J, Ainsworth S, Nauta A, van Sinderen D 2013) **Bacteriophage orphan DNA methyltransferases: insights from their bacterial origin, function, and occurrence** *Applied and environmental microbiology* **79**:7547–7555

79. Iida S, Streiff MB, Bickle TA, Arber W 1987) **Two DNA antirestriction systems of bacteriophage P1, darA, and darB: characterization of darA– phages** *Virology* **157**:156–166

80. Kvitko BH, Collmer A 2011) **Construction of Pseudomonas syringae pv. tomato DC3000 mutant and polymutant strains** *Methods Mol Biol* **712**:109–28

81. Xie Q, Wu TP, Gimple RC, Li Z, Prager BC, Wu Q, Yu Y, Wang P, Wang Y, Gorkin DU 2018) **N6-methyladenine DNA modification in glioblastoma** *Cell* **175**:1228–1243

82. Kim D, Langmead B, Salzberg SL 2015) **HISAT: a fast spliced aligner with low memory requirements** *Nat Methods* **12**:357–60

83. Love MI, Huber W, Anders S 2014) **Moderated estimation of fold change and dispersion for RNA-seq data with DESeq2** *Genome biology* **15**:1–21

84. Yu G, Wang L-G, Han Y, He Q-Y 2012) **clusterProfiler: an R package for comparing biological themes among gene clusters** *Omics: a journal of integrative biology* **16**:284–287

85. Hua C, Huang J, Wang T, Sun Y, Liu J, Huang L, Deng X 2022) **Bacterial Transcription Factors Bind to Coding Regions and Regulate Internal Cryptic Promoters** *mBio* **13**

86. Xiao Y, Lan L, Yin C, Deng X, Baker D, Zhou JM, Tang X 2007) **Two-component sensor RhpS promotes induction of Pseudomonas syringae type III secretion system by repressing negative regulator RhpR** *Mol Plant Microbe Interact* **20**:223–34

87. Shao X, Xie Y, Zhang Y, Deng X 2019) **Biofilm Formation Assay in Pseudomonas syringae** *Bio Protoc* **9**

Author information

Jiadai Huang[#]
Department of Biomedical Sciences, City University of Hong Kong, Hong Kong, China

[#]These authors contributed equally to the paper as the first authors.

Fang Chen[#]
Department of Biomedical Sciences, City University of Hong Kong, Hong Kong, China

[#]These authors contributed equally to the paper as the first authors.

Beifang Lu
Department of Biomedical Sciences, City University of Hong Kong, Hong Kong, China

Yue Sun
Department of Biomedical Sciences, City University of Hong Kong, Hong Kong, China

Youyue Li
Department of Biomedical Sciences, City University of Hong Kong, Hong Kong, China

Canfeng Hua
Department of Biomedical Sciences, City University of Hong Kong, Hong Kong, China

Xin Deng
Department of Biomedical Sciences, City University of Hong Kong, Hong Kong, China, Shenzhen Research Institute, City University of Hong Kong, Shenzhen, China, Tung Research Centre, City University of Hong Kong, Hong Kong SAR, China, Chengdu Research Institute, City University of Hong Kong, Chengdu, China
ORCID iD: 0000-0003-1580-0089

For correspondence: xindeng@cityu.edu.hk

Editors

Reviewing Editor
Bavesh Kana
University of the Witwatersrand, Johannesburg, South Africa

Senior Editor
Bavesh Kana
University of the Witwatersrand, Johannesburg, South Africa

Reviewer #1 (Public review):

Summary:

In this work, Huang et al used SMRT sequencing to identify methylated nucleotides (6mA, 4mC, and 5mC) in Pseudomonas syringae genome. They show that the most abundant modification is 6mA and they identify the enzymes required for this modification as when they mutate HsdMSR they observe a decrease of 6mA. Interestingly, the mutant also displays phenotypes of change in pathogenicity, biofilm formation, and translation activity due to a change in gene expression likely linked to the loss of 6mA.

Overall, the paper represents an interesting set of new data that can bring forward the field of DNA modification in bacteria.

Comments on revisions:

Thank you for the additional work. The authors have now addressed all my concerns.

https://doi.org/10.7554/eLife.96290.2.sa2

Reviewer #2 (Public review):

In the present manuscript, Huang et.al. revealed the significant roles of the DNA methylome in regulating virulence and metabolism within Pseudomonas syringae, with a particular focus on the HsdMSR system in this model strain. The authors used SMRT-seq to profile the DNA methylation patterns (6mA, 5mC, and 4mC) in three P. syringae strains (Psph, Pss, and Psa) and displayed the conservation among them. They further identified the type I restriction-modification system (HsdMSR) in P. syringae, including its specific motif sequence. The HsdMAR participated in the process of metabolism and virulence (T3SS & Biofilm formation), as demonstrated through RNA-seq analyses. Additionally, the authors revealed the mechanisms of the transcriptional regulation by 6mA. Strictly from the point of view of the interest of the question and the work carried out, this is a worthy and timely study that uses third-generation sequencing technology to characterize the DNA methylation in P. syringae. The experimental approaches were solid, and the results obtained were interesting and provided new information on how epigenetics influences the transcription in P. syringae. The conclusions of this paper are mostly well supported by data.

Comments on revisions:

The authors have successfully addressed all the comments from the reviewers in their revised manuscript.

https://doi.org/10.7554/eLife.96290.2.sa1

Author response:

The following is the authors' response to the original reviews.

> ***Public Reviews:***
>
> ***Reviewer #1 (Public Review):***
>
> *Summary:*
>
> *In this work, Huang et al used SMRT sequencing to identify methylated nucleotides (6mA, 4mC, and 5mC) in Pseudomonas syringae genome. They show that the most abundant modification is 6mA and they identify the enzymes required for this modification as when they mutate HsdMSR they observe a decrease of 6mA. Interestingly, the mutant also displays phenotypes of change in pathogenicity, biofilm formation, and translation activity due to a change in gene expression likely linked to the loss of 6mA. Overall, the paper represents an interesting set of new data that can bring forward the field of DNA modification in bacteria.*

Thank you for your valuable feedback on our paper exploring the impact of 6mA modification in P. syringae.

> *Major Concerns:*

> *Most of the authors' data concern Psph pathovar. I am not sure that the authors' conclusions are supported by the two other pathovars they used in the initial 2 figures. If the authors want to broaden their conclusions to Pseudomonas syringe and not restrict it to Psph, the authors should have stronger methylation data using replicates. Additionally, they should discuss why Pss is so different than Pst and Psph. Could they do a blot to confirm it is really the case and not a sequencing artifact? Is the change of methylation during bacterial growth conserved between the pathovar? The authors should obtain mutants in the other pathovar to see if they have the same phenotype. The authors have a nice set of data concerning Psph but the broadening of the results to other pathovar requires further investigation.*

We appreciate the reviewer's insightful comments. While the majority of our data focuses on the Psph, we recognize the importance of validating these findings in Pss and Pst. To this end, we have performed additional experiments using dot blot and mutant construction to enhance our conclusions in other pathovars.

We agree that we should discuss why Pss is different from Psph and Pst. We performed a dot blot assay using genome DNA in Pss and Pst, presented in Figure S5A. Meanwhile, we compared the 6mA modification level of Pss and Pst in different growth phases. As shown in Figure S5A, the change of methylation during bacterial growth is conserved in Pst. The change was not obvious in Pss, which might be due to the lack of a type I R-M system.

"In accordance with previous studies showing that growth conditions affect the bacterial methylation status, we applied dot blot experiments using the same amount of DNA (1 μg) from these three P. syringae strains to detect the 6mA levels during both logarithmic and stationary phases. The results revealed that 6mA levels in the stationary phase were much higher compared to the logarithmic phase in Psph and Pst, but no significant change in Pss. Additionally, we found that during the stationary phase, 6mA methylation levels in Psph and Pst were higher than those in Pss. These findings were consistent with the MTases predication on these three strains, since Pss does not harbor any type I R-M systems, which are important for 6mA medication in bacteria."

Please see Figure S5A and Lines 220-228 in the revised manuscript.

We also tried to construct an HsdM mutant in Pst to explore whether the influence of 6mA methylation was conserved in P. syringae, but it failed after multiple attempts. We did not construct a Pss mutant because no type I R-M system was predicted, and few methylation sites were identified via SMRT-seq in this strain. Therefore, we overexpressed HsdM in Pst instead. We have performed additional experiments in WT and the HsdM overexpression strains, including dot blot and growth curve assays.

Please see Figures S5B-C and Lines228-232 in the revised manuscript.

> *The authors should include proper statistical analysis of their data. A lot of terms are descriptive but not supported by a deeper analysis to sustain the conclusions. For example, in Figure 4E, we do not know if the overlap is significant or not. Are DEGs more overlapping to 6mA sites than non-DEGs? Here is a non-exhaustive list of terms that need to be supported by statistics: different level (L145), greater conservation (L162), significant conservation (L165), considerable similarity (L175), credible motifs (L189), Less strong (L277) and several "lower" and "higher" throughout the text.*

Thank you for the insightful feedback. We have made the following revisions in the manuscript to ensure that the terms are more precise and do not require statistical significance testing.

(1) Statistical analysis: We have added statistical tests for the overlap between DEGs and 6mA sites in Figure 4E. We performed the Fisher test, and we found the overlap was not significant (p> 0.05). DEGs and non-DEGs were both non-significant overlapped 6mA sites. Please see Figure 4E and Lines 261-262.

“Less strong” was used to indicate the influence of HsdM on biofilm in Figure 5D. All Figures with “*” labels were analyzed using students' two-tailed t-tests with a significant change ($p < 0.05$).

(2) Revised wording: For terms used to describe comparisons, we have revised the wording to be clearer and ensure that the terminology used did not imply the need for statistical significance testing when not required. For example:

“Different level” has been removed. Please see Lines 143-144.

“Greater conservation” has been revised to “more conserved functional terms”. Please see Lines 161-162.

“Significant conservation” has been revised to “notable conservation”. Please see Line 165.

“Credible motifs” has been revised to “identified motifs”. Please see Line 186.

> *The authors performed SMRT sequencing of the delta hsdMSR showing a reduction of 6mA. Could they include a description of their results similar to Figures 1-2. How reduced is the 6mA level? Is it everywhere in the genome? Does it affect other methylation marks? This analysis would strengthen their conclusions.*

Yes, we agree. We have provided additional analysis and descriptions to strengthen the conclusions regarding these valuable comments. We determined three methylation sites in the HsdMSR mutant strain and compared the overlapped genes within these modification patterns. Specifically, we focused on the 6mA sites in Psph WT, HsdMSR mutant, and HsdM motif $CAGCN_{(6)}CTC$. As expected, we found almost all of the reduction 6mA sites in the ΔhsdMSR were from motif $CAGCN_{(6)}CTC$. We also noticed that 5mC and 4mC sites in the mutant were relatively similar to that in WT, and the slight difference might be caused by sequencing errors. Overall, we propose that HsdMSR only catalyze the 6mA located on the motif $CAGCN_{(6)}CTC$, but does not affect other 6mA sites and other modification types.

Please see Figures S4D-E and Lines 212-218 in the revised manuscript.

> *In Figure 6E to conclude that methylation is required on both strands, the authors are missing the control CAGCN6CGC construct otherwise the effect could be linked to the A on the complementary strand.*

Thank you for your valuable suggestions. We have provided the control result on the complementary strand. Please see Figure 6C. The new result evidences the conclusion that 6mA methylation regulates gene transcription based on methylation on both strands.

Please see Figure 6C and Lines 329-330 in the revised manuscript.

> ***Reviewer #2 (Public Review):***
>
> *In the present manuscript, Huang et.al. revealed the significant roles of the DNA methylome in regulating virulence and metabolism within Pseudomonas syringae, with a particular focus on the HsdMSR system in this model strain. The authors used SMRT-seq to profile the DNA methylation patterns (6mA, 5mC, and 4mC) in three P. syringae strains (Psph, Pss, and Psa) and displayed the conservation among them. They further identified*

> *the type I restriction-modification system (HsdMSR) in P. syringae, including its specific motif sequence. The HsdMAR participated in the process of metabolism and virulence (T3SS & Biofilm formation), as demonstrated through RNA-seq analyses. Additionally, the authors revealed the mechanisms of the transcriptional regulation by 6mA. Strictly from the point of view of the interest of the question and the work carried out, this is a worthy and timely study that uses third-generation sequencing technology to characterize the DNA methylation in P. syringae. The experimental approaches were solid, and the results obtained were interesting and provided new information on how epigenetics influences the transcription in P. syringae. The conclusions of this paper are mostly well supported by data, but some aspects of data analysis and discussion need to be clarified and extended.*

Thank you for your positive feedback and recognition of the importance of our study. We appreciate the suggestions for further clarification and extension of some aspects of data analysis and discussion. We added further analysis of the SMRT-seq result of the ΔhsdMSR and overexpressed HsdM in Pst to provide more information on conservation. We added these contents to the discussion in the revised manuscript. Please see Figure 6C and Figure S5.

> ***Reviewer #3 (Public Review):***
>
> *Summary:*
>
> *The article by Huang et.al. presents an in-depth study on the role of DNA methylation in regulating virulence and metabolism in Pseudomonas syringae, a model phytopathogenic bacterium. This comprehensive research utilized single-molecule real-time (SMRT) sequencing to profile the DNA methylation landscape across three model pathovars of P. syringae, identifying significant epigenetic mechanisms through the Type-I restriction-modification system (HsdMSR), which includes a conserved sequence motif associated with N6-methyladenine (6mA). The study provides novel insights into the epigenetic mechanisms of P. syringae, expanding the understanding of bacterial pathogenicity and adaptation. The use of SMRT sequencing for methylome profiling, coupled with transcriptomic analysis and in vivo validation, establishes a robust evidence base for the findings*
>
> *Strengths:*
>
> *The results are presented clearly, with well-organized figures and tables that effectively illustrate the study's findings.*
>
> *Weaknesses:*
>
> *It would be helpful to add more details, especially in the methods, which make it easy to evaluate and enhance the manuscript's reproducibility.*

Thank you for the positive evaluation of our study, as well as the constructive feedback provided. We have added more details in methods for RNA-seq analysis and Ribo-seq analysis. Please see Lines 484-515.

“Briefly, bacteria were cultured to an OD_{600} of 0.4, at which point chloramphenicol was added to a final concentration of 100 μg/mL for 2 minutes. Cells were then pelleted and washed with pre-chilled lysis buffer [25 mM Tris-HCl, pH 8.0; 25 mM NH4Cl; 10 mM MgOAc; 0.8% Triton X-100; 100 U/mL RNase-free DNase I; 0.3 U/mL Superase-In; 1.55 mM chloramphenicol; and 17 mM GMPPNP]. The pellet was resuspended in lysis buffer, followed by three freeze-thaw cycles using liquid nitrogen. Sodium deoxycholate was then added to a final concentration of 0.3% before centrifugation. The resulting supernatant was adjusted to 25 A260 units and mixed with 2 mL of 500 mM $CaCl_2$ and 12 μL MNase, making up a total

volume of 200 µL. After the digestion, the reaction was quenched with 2.5 mL of 500 mM EGTA. Monosomes were isolated using Sephacryl S400 MicroSpin columns, and RNA was purified using the miRNeasy Mini Kit (Qiagen). rRNA was removed using the NEBNext rRNA Depletion Kit, and the final library was constructed with the NEBNext Small RNA Library Prep Kit. For each sample, ribosome footprint reads were mapped to the Psph 1448A reference genome, and the translational efficiency was calculated by dividing the normalized Ribo-seq counts by the normalized RNA counts. Two biological replicates were performed for all experiments."

> ***Recommendations For The Authors:***
>
> ***Reviewer #1 (Recommendations For The Authors):***
>
> *I would recommend the authors limit their manuscript to Psph pathovar and include statistical analysis supporting their conclusions.*

Thank you for your suggestion.

> *Minor*
>
> *• L104: "significantly" please add a p-value and explain the analysis.*

Sorry for the confusion. We have added the p-value and explained the analysis in the method section. The p-value used for SMRT-seq was the modification quality value (QV) score, which were used to call the modified bases A (QV=50) and C (QV=100). Please see Lines 452-454.

> *• Figures 1B, D, F, and Figure 2A: make the Venn diagram to scale*

Yes, we have revised.

> *• L110-111: missing p-value to say that the authors observe a bigger overlap in Pst than Psph as they observed more modified sites in Pst*

Sorry for the confusion. We said it had a bigger overlap in Pst because the number 17.7 was bigger than the number of 15 in Psph. To avoid misunderstanding, we revised the wording to "more genes equipped with all three modification types were detected in Pst than Psph". Please see Lines 110-111.

> *• L112: missing description of their Pss analysis (IDP, sites...)*

We have added the information for Pss in the revised manuscript.

"Additionally, the methylome atlas of Pss revealed a lower incidence of methylation than those of Psph and Pst, particularly in terms of 6mA modifications, which were only seen in 457 significant 6mA occurrences under the same threshold (IPD > 1.5) and a total of 2,853 and 1,438 methylation sites were detected as 5mC and 4mC, respectively". Please see Lines 114-116.

> *• L118: "modification" to "modified "*

We have revised. Please see Line 119.

> *• L120: "modification sites" to "modified nucleotides"*

We have revised. Please see Line 121.

> *• L142: correct the title "Methylated genes revealed highly functional conservation among three P. syringae strains" maybe to "Methylated genes are functionally conserved among ..."*

We have revised. Please see Line 142.

> *• Figure 2C: not easy to read and interpret*

Sorry for the confusion. Figure 2C revealed the significantly enriched functional pathways in GO and KEGG databases among three P. syringae strains. The specific names of each pathway were listed on the left, and each column with dots indicated the number of genes within one kind of methylation in one of three P. syringae strains. The larger the size, the bigger the number.

We have revised the legend of Figure 2C. Please see Lines 575-579.

“The dot plot revealed the significantly enriched functional pathways in GO and KEGG databases among three P. syringae strains. The specific names of each pathway were listed on the left, and each column with dots indicated the number of genes within one kind of methylation in one of three P. syringae strains. The size of the dots indicates the number of related genes.”

> *• Figure 6B-C: what is the difference between B 24h and C?*

Figure 6B revealed the expression difference between WT and mutant during 24 hours. Figure 6C only showed a time point in 24 hours. To avoid repetition, we have removed Figure 6C.

> *• Figure 6C-D: if the same maybe remove Figure 2C*

We have removed Figure 6D.

> ***Reviewer #2 (Recommendations For The Authors):***
>
> *The manuscript could be improved by addressing the following concerns:*
>
> *(1) In line 146: How to understand the percentage conserved in "more than two of the strains"?*

Sorry for the confusion, we planned to indicate the pattern that conserved in two strains and three strains. We have revised it to: “Notable, about 25% to 45% of methylated genes were conserved in two and three strains”. Please see Line 145.

> *(2) In line 178: Five conserved sequence motifs should be replaced by "Six conserved sequence motifs".*

We have revised. Please see Line 176.

> *(3) In Figure 2B, specify the C1, C2 and C3. "m6A" should be replaced by "6mA".*

Yes, we have revised.

> *(4) In Figure S2, "m6A" should be replaced by "6mA".*

Yes, we have revised.

> *(5) In line 212, please add references for the previous studies showing that growth conditions affect bacterial methylation status.*

Thank you for your suggestion. We have added the relevant references (Gonzalez and Collier, 2013), (Krebes et al., 2014), (Sanchez-Romero and Casadesus, 2020).

> *(6) In line 217, "illustrate" should be "illustrated".*

Yes, we have revised. Please see Line 210.

> *(7) There are some genes colored in grey, revealing bigger differences between the two strains than those related to ribosomal protein, T3SS, and alginate synthesis in Fig. 4A. Do they have important functional roles as well?*

Thank you for your suggestion. A total of 116 genes with bigger differences ($|\mathrm{Log_2FC}| > 2$) except for genes related to ribosomal protein, T3SS, and alginate synthesis. Among these genes, 31 were annotated as hypothetical proteins and 4 as transcription factors with unknown functions, and the remaining genes mostly encoded metabolism-related enzymes. These enzymes might have effects on growth defects in ΔhsdMSR. We added this information in the revised manuscript. Please see Line 249-254.

> *(8) The authors should discuss what will be the potential signals or factors that can regulate the activity of HsdMSR. In other words, what can decide the extent of methylation through activating or suppressing the expression of HsdMSR?*

Thank you for your valuable suggestion. We have added this part in the discussion part. Please see Lines 404-415.

“Apart from the established roles of 6mA and HsdMSR in P. syringae, certain signals or factors may influence HsdMSR expression. For instance, we confirmed that the growth phase affects methylation levels in P. syringae. Previous studies have shown that increased temperatures can reduce methylation levels, as observed in PAO1(Doberenz et al., 2017). These findings suggest that HsdMSR expression may be responsive to both intrinsic cellular states and extrinsic environmental conditions. To further explore potential upstream TFs regulating the expression of HsdMSR, we searched for TF-binding sites in the HsdMSR promoter using our own databases (Fan et al., 2020; Shao et al., 2021; Sun et al., 2024). As a result, we found three candidate TFs (PSPPH_0061, PSPPH_3268, and PSPPH_3504) that might directly bind and regulate HsdMSR expression. Future studies on these TFs and their interactions with the HsdMSR promoter would help clarify the regulatory network governing HsdMSR activity.”

> ***Reviewer #3 (Recommendations For The Authors):***
>
> *(1) Some figures contain dense information, which may be overwhelming for readers. Streamlining the legend for Figure 1 and resizing the Venn diagrams within it could enhance clarity and visual appeal.*

Thank you for your suggestion. We have scaled all the Venn plots in the revised version.

> *(2) Incorporating a discussion about the role of the restriction-modification (RM) system in bacterial defense against phage infection into the discussion section could enrich the manuscript's context and relevance.*

Thank you for your valuable suggestion. We have added this part in the Discussion part. Please see Lines 416-427.

“RM systems are known for their intrinsic role as innate immune systems in anti-phage infection, and present in around 90% of bacterial genomes(Oliveira et al., 2014). RM systems protect bacteria self by recognizing and degrading foreign phage DNA via methylation-specific site and restriction endonucleases (REases) (Loenen et al., 2014). In addition, other phage-resistance systems are similar to RM systems but carry extra genes. One is called the phage growth limitation (Pgl) system, which modifies and cleaves phage DNA. However, the Pgl only modifies the phage DNA in the first infection cycle, and cleaves phage DNA in the subsequent infections, which gives a warn to the neighboring cells(Hampton et al., 2020; Hoskisson et al., 2015). To counteract RM and RM-like systems, phages have evolved strategies, including unusual modifications such as hydroxymethylation, glycosylation, and glucosylation. They can also encode their own MTases to protect their DNA or employ strategies to evade restriction systems and other anti-RM defenses.(Iida et al., 1987; Murphy et al., 2013; Vasu and Nagaraja, 2013).

> *(3) In line 152: What is the importance of the mentioned example of Cro/CI family TF?*

Thank you for your comments. The Cro/CI are important TFs present in phages. The interaction between Cro and CI affects bacteria immunity status in Enterohemorrhagic Escherichia coli (EHEC) strains(Jin et al., 2022). RM systems are known as a kind of phage-defense system, and hence we mentioned it here. We have added this description in the revised manuscript. Please see Lines 152-154.

Reference:

(1) Doberenz, S., Eckweiler, D., Reichert, O., Jensen, V., Bunk, B., Sproer, C., Kordes, A., Frangipani, E., Luong, K., Korlach, J., et al. (2017). Identification of a Pseudomonas aeruginosa PAO1 DNA Methyltransferase, Its Targets, and Physiological Roles. mBio 8. 10.1128/mBio.02312-16.

(2) Fan, L., Wang, T., Hua, C., Sun, W., Li, X., Grunwald, L., Liu, J., Wu, N., Shao, X., Yin, Y., et al. (2020). A compendium of DNA-binding specificities of transcription factors in Pseudomonas syringae. Nat Commun 11, 4947. 10.1038/s41467-020-18744-7.

(3) Gonzalez, D., and Collier, J. (2013). DNA methylation by CcrM activates the transcription of two genes required for the division of Caulobacter crescentus. Mol Microbiol 88, 203-218. 10.1111/mmi.12180.

(4) Hampton, H.G., Watson, B.N., and Fineran, P.C. (2020). The arms race between bacteria and their phage foes. Nature 577, 327-336.

(5) Hoskisson, P.A., Sumby, P., and Smith, M.C. (2015). The phage growth limitation system in Streptomyces coelicolor A (3) 2 is a toxin/antitoxin system, comprising enzymes with DNA methyltransferase, protein kinase and ATPase activity. Virology 477, 100-109.

(6) Iida, S., Streiff, M.B., Bickle, T.A., and Arber, W. (1987). Two DNA antirestriction systems of bacteriophage P1, darA, and darB: characterization of darA− phages. Virology 157, 156-166.

(7) Jin, M., Chen, J., Zhao, X., Hu, G., Wang, H., Liu, Z., and Chen, W.-H. (2022). An engineered λ phage enables enhanced and strain-specific killing of enterohemorrhagic Escherichia coli. Microbiology Spectrum 10, e01271-01222.

(8) Krebes, J., Morgan, R.D., Bunk, B., Sproer, C., Luong, K., Parusel, R., Anton, B.P., Konig, C., Josenhans, C., Overmann, J., et al. (2014). The complex methylome of the human gastric

pathogen Helicobacter pylori. Nucleic Acids Res 42, 2415-2432. 10.1093/nar/gkt1201.

(9) Loenen, W.A., Dryden, D.T., Raleigh, E.A., Wilson, G.G., and Murray, N.E. (2014). Highlights of the DNA cutters: a short history of the restriction enzymes. Nucleic Acids Res 42, 3-19.

(10) Murphy, J., Mahony, J., Ainsworth, S., Nauta, A., and van Sinderen, D. (2013). Bacteriophage orphan DNA methyltransferases: insights from their bacterial origin, function, and occurrence. Appl Environ Microb 79, 7547-7555.

(11) Oliveira, P.H., Touchon, M., and Rocha, E.P. (2014). The interplay of restriction-modification systems with mobile genetic elements and their prokaryotic hosts. Nucleic Acids Res 42, 10618-10631.

(12) Sanchez-Romero, M.A., and Casadesus, J. (2020). The bacterial epigenome. Nature reviews. Microbiology 18, 7-20. 10.1038/s41579-019-0286-2.

(13) Shao, X., Tan, M., Xie, Y., Yao, C., Wang, T., Huang, H., Zhang, Y., Ding, Y., Liu, J., Han, L., et al. (2021). Integrated regulatory network in Pseudomonas syringae reveals dynamics of virulence. Cell Rep 34, 108920. 10.1016/j.celrep.2021.108920.

(14) Sun, Y., Li, J., Huang, J., Li, S., Li, Y., Lu, B., and Deng, X. (2024). Architecture of genome-wide transcriptional regulatory network reveals dynamic functions and evolutionary trajectories in Pseudomonas syringae. bioRxiv, 2024.2001. 2018.576191.

(15) Vasu, K., and Nagaraja, V. (2013). Diverse functions of restriction-modification systems in addition to cellular defense. Microbiol Mol Biol Rev 77, 53-72. 10.1128/MMBR.00044-12.

https://doi.org/10.7554/eLife.96290.2.sa0